

GEOLOGY OF THE MODOC Pb-Ag-Zn DISTRICT,  
INYO COUNTY, CALIFORNIA

A Thesis Submitted to the Faculty of the Graduate School  
of the University of Minnesota

by

DANIEL LEE ENGLAND

In Partial Fulfillment of the Requirements  
for the Degree of  
Master of Science

May 1986

## ABSTRACT

The Modoc District, in Central Inyo County, California is underlain by a 1600 meter sequence of Devonian to Permian marine carbonate rocks. These have been intruded by a quartz monzonite stock of Jurassic age and a swarm of andesite porphyry dikes of Cretaceous (?) age. Late Cenozoic olivine basalt flows and sedimentary deposits unconformably overlie the older rocks.

Three distinct zones of contact metamorphism are developed within the carbonate strata as an aureole around the quartz monzonite stock. These zones are divided on the basis of their characteristic mineral assemblages and consist of: a) an albite-epidote hornfels facies zone (2.5 km to 700 meters away from the intrusive contact), b) a hornblende-hornfels facies zone (approximately 700 to 30 meters away), and c) a pyroxene-hornfels facies zone (30 meters away up to the contact itself).

Structurally controlled Pb-Ag-Zn ore of the district is in marble of Devonian and Mississippian ages; whereas, silty limestone of Pennsylvanian and Permian ages appear unfavorable for ore development. The ore bodies are small but high grade. Argentiferous galena with exsolution blebs of tetrahedrite are the principal primary ore minerals. Secondary ore is manganese-rich, and contains cerussite, hemimorphite, cerargyrite and relict galena. High silver grades are encountered throughout many of the deposits with the primary source of the silver being within galena as  $Ag_2S$ , and within tetrahedrite as a solid solution between tetrahedrite-freibergite series minerals. Dolomitization of the marble, formation of

manganese minerals, and the occasional addition of silica, are the common wall rock alterations associated with ore mineralization; this alteration is not widespread.

It is envisioned that hydrothermal solutions of connate/meteoric origin were set into convective circulation by the heat generated from the quartz-monzonite stock. These water-rich saline solutions leached metals from the country rock, carrying them in chloride complexes. As these hydrothermal solutions migrated upward, their temperature and salinity decreased, and their pH increased, thus precipitating out the metals in structurally prepared zones and mineralizing the Devonian and Mississippian marble of the district.

## ACKNOWLEDGEMENTS

I would first like to acknowledge Lacana Mining Incorporated's Reno office for originally suggesting, and financially supporting, this thesis. They were a constant source of helpful cooperation. In this regard, Mike Fiannaca deserves special mention.

The professional assistance of the faculty and staff of the University of Minnesota - Duluth Geology Department, was invaluable. I especially benefited from the advice and various consultations with Dr. Ron Morton, my major advisor, and Dr.s James Grant and Richard Ojakangas, who served as members of my thesis committee.

Special thanks are extended to Cathy Leece, who spent endless hours typing, revising and drafting. Without her help the final draft of this thesis would not have been completed.

Finally, I would like to acknowledge the constant encouragement of my parents, Bernice and Joseph, to whom I dedicate this work.

## TABLE OF CONTENTS

ABSTRACT . . . . .	i
ACKNOWLEDGEMENTS . . . . .	iii
TABLE OF CONTENTS . . . . .	iv
ILLUSTRATIONS . . . . .	vi
Figures . . . . .	vi
Tables . . . . .	viii
Plates . . . . .	viii
INTRODUCTION . . . . .	1
Purpose of Study . . . . .	1
Location, Access, and Physiography . . . . .	2
Methods of Study . . . . .	4
Previous Work . . . . .	6
Regional Geology . . . . .	8
LITHOLOGY AND STRATIGRAPHY . . . . .	12
Paleozoic Rocks . . . . .	12
General Features . . . . .	12
Devonian System . . . . .	14
Lost Burro Formation . . . . .	14
Mississippian System . . . . .	18
Tin Mountain Formation . . . . .	18
Perdido Formation . . . . .	20
Mississippian and Pennsylvanian System . . . . .	23
Lee Flat Limestone . . . . .	23
Pennsylvanian System . . . . .	25
Lower Unit Keeler Canyon Formation . . . . .	25
Mesozoic Rocks . . . . .	27
Biotite-Hornblende-Quartz Monzonite . . . . .	27
Other Intrusive Rocks (Pods or Dikes) . . . . .	28
Altered Andesite Porphyry Dikes . . . . .	30
Cenozoic Rocks . . . . .	33
Olivine Basalt . . . . .	33
Quartz Porphyry Dike . . . . .	34
METAMORPHISM AND ALTERATION . . . . .	38
Metamorphism and Alteration of Limestones . . . . .	38
Introduction . . . . .	38
Formation of Calc-Silicate Minerals (Zones 1 and 2) . . . . .	40
Alteration to Skarn and Calc-Silicate Hornfels (Zone 3) . . . . .	41
Conditions of Metamorphism . . . . .	45
Dolomitization . . . . .	50
Metasomatism Within the Quartz Monzonite Stock . . . . .	52

STRUCTURE . . . . .	55
Introduction . . . . .	55
Folds . . . . .	55
Faults . . . . .	57
LEAD, SILVER, ZINC ORE DEPOSITS . . . . .	60
Distribution . . . . .	60
Size and Character of Ore Bodies . . . . .	60
Mineralogy . . . . .	61
Hypogene Minerals . . . . .	63
Gangue Minerals . . . . .	63
Supergene Minerals . . . . .	66
Primary Source of the Silver . . . . .	68
Ore Controls . . . . .	69
Wall Rock Alteration . . . . .	70
Model of Ore Genesis . . . . .	74
CONCLUSIONS . . . . .	77
REFERENCES CITED . . . . .	80
APPENDIX A: Modal Compositions of Rock Units . . . . .	A-1
APPENDIX B: Modal Compositions of Ore Samples . . . . .	A-9
APPENDIX C: Analyses of Assayed Samples . . . . .	A-11
APPENDIX D: Chemical Analyses of Igneous Rocks . . . . .	A-14

ILLUSTRATIONS

<u>Figure</u>	<u>Page</u>
1. Location map of study area . . . . .	3
2. Map of regional geology . . . . .	9
3. Index map of quadrangle locations . . . . .	11
4. Stratigraphic section of the Modoc District . . . . .	13
5. East side of Lookout Mountain, showing Lost Burro Formation	16
6. Limestone and marble beds of Lost Burro Formation . . . . .	16
7. Photomicrograph of Lost Burro limestone showing tremolite grains in a matrix of calcite . . . . .	17
8. Photomicrograph of Lost Burro marble with cross-cutting quartz veins . . . . .	17
9. Tin Mountain Formation, showing chert nodules in limestone .	19
10. Photomicrograph showing shear foliation in the Tin Mountain Formation . . . . .	19
11. Alternating chert and silty micrite beds in the Perdido Formation . . . . .	22
12. Massive white marble of the Lee Flat Formation . . . . .	24
13. Photomicrograph of sparry calcite grains of the Lee Flat Formation . . . . .	24
14. Keeler Canyon Formation with chert nodules . . . . .	26
15. Photomicrograph of silty micrite with cross-cutting, sparry calcite veins . . . . .	26
16. Photomicrograph of biotite-hornblende-quartz monzonite . . .	29
17. Altered andesite dikes, within fault zone, cross-cutting the Lost Burro Formation . . . . .	32
18. Olivine basalt lava flow with flow lineations . . . . .	35
19. Photomicrograph of olivine basalt flow showing altered olivine phenocrysts . . . . .	35
20. Quartz porphyry dike cross-cutting the Perdido Formation . .	36

<u>Figure</u>	<u>Page</u>
21. Photomicrograph of K-feldspar, quartz and muscovite in a felty groundmass in the quartz porphyry dike . . . . .	37
22. Map of contact metamorphic zone distribution . . . . .	39
23. Reactions for the formation of calc-silicate minerals . . . . .	42
24. Photomicrograph of hornfels composed of wollastonite, diopside, calcite and garnet . . . . .	44
25. Photomicrograph of an idocrase grain showing color zonation . . . . .	44
26. Photomicrograph of skarn mineralization in the Tin Mountain Formation (idocrase, diopside, calcite) . . . . .	46
27. Photomicrograph of skarn mineralization in the Tin Mountain Formation (wollastonite, diopside, calcite, garnet) . . . . .	46
28. Mole fraction CO <sub>2</sub> versus temperature diagram . . . . .	47
29. ACF diagram of mineral assemblages in zone 3 . . . . .	49
30. Irregular shaped zone of dolomitization within the Lost Burro Formation . . . . .	51
31. Photomicrograph of altered quartz monzonite near contact with Perdido Formation . . . . .	53
32. Map of structural geology of the Modoc District . . . . .	56
33. The major anticline within the Tin Mountain Formation . . . . .	58
34. Drag folding within the Lost Burro Formation . . . . .	58
35. Photomicrograph of tetrahedrite exsolution blebs in galena . . . . .	64
36. Photomicrograph of sphalerite grain in galena . . . . .	65
37. Photomicrograph of pyrite grains in galena . . . . .	65
38. Photomicrograph of replacement texture between galena and gangue . . . . .	67
39. Photomicrograph of covelite and chalcocite in galena . . . . .	67
40. Photomicrograph of dolomite in alteration zones adjacent to Ag ore within the Lost Burro Formation . . . . .	72
41. Photomicrograph of dolomite vein in calcite . . . . .	72



<u>Figure</u>	<u>Page</u>
42. Mole fraction of Ca / Ca + Mg versus temperature diagram . .	73

Table .

I. Chemical analyses of the quartz monzonite stock . . . . .	54
II. Minerals identified within the Pb-Ag-Zn deposits . . . . .	62
III. Modal compositions of the Lost Burro Formation . . . . .	A-2
IV. Modal compositions of the Tin Mountain Formation . . . . .	A-3
V. Modal compositions of the Perdido Formation . . . . .	A-4
VI. Modal compositions of Lee Flat limestone . . . . .	A-5
VII. Modal compositions of the Keeler Canyon Formation . . . . .	A-5
VIII. Modal compositions of hornblende-biotite-quartz monzonite	A-6
IX. Modal compositions of quartz porphyry dike . . . . .	A-7
X. Modal compositions of andesite dikes . . . . .	A-7
XI. Modal compositions of olivine basalt . . . . .	A-7
XII. Modal compositions of other intrusives . . . . .	A-8
XIII. Modal compositions of polished ore samples . . . . .	A-10
XIV. Chemical analyses of igneous rocks . . . . .	A-14

Plate

1. Geology map of the Modoc Pb-Ag-Zn District . . . . .	pocket
---	--------

## INTRODUCTION

### PURPOSE OF STUDY

The occurrence of Pb, Ag, Zn deposits within Paleozoic carbonate strata near granitic intrusions has long been recognized in southeastern California. This relationship, in the Modoc District, Inyo County, California, though previously noted (Waring and Hugvenin, 1919; Tucker and Sampson, 1938; Hall and Stephens, 1963), has never been studied in detail. The purpose of this thesis is to examine this relationship within the Modoc District by:

- 1) Studying changes in mineralogy, textural relationships, and structures of both mineralized and non-mineralized carbonate rocks;
- 2) Studying alteration as it relates to contact metamorphism and/or ore formation;
- 3) Studying ore controls as they relate to intrusive contacts, stratigraphy, structure, and contact metasomatism;
- 4) Classifying the ore deposits and developing possible models of ore genesis.

## LOCATION, ACCESS, AND PHYSIOGRAPHY

The Modoc District is located in Central Inyo County, Southeastern California. It is situated on the northeastern flank of the Argus Mountain Range just west of the Panamint Valley (Figure 1).

Access to the district is provided by a) State Highway 190, which extends from U.S. Highway 6 in Owens Valley to Death Valley, and b) a paved county road from the town of Trona. Trona and Lone Pine, 38 miles south and 46 miles west of the district respectively, are the closest populated centers. The district proper is most easily negotiated with a four-wheel-drive vehicle via dirt roads that join the Modoc, Minnietta and Defense Mine sites (Plate 1).

Topography of the district is steep, with relief ranging from 670 to 1650 meters. Locally, slopes average  $40^{\circ}$  to  $57^{\circ}$ , making the difficulty of traverse tremendous.

Vegetation is sparse, with steep, essentially bare, slopes. The climate is typically arid and is characterized by a large range in temperature and frequent high winds. This lack of vegetation and absence of any soil horizon makes outcrop exposure, for all practical purposes, 100%.

# Location Map

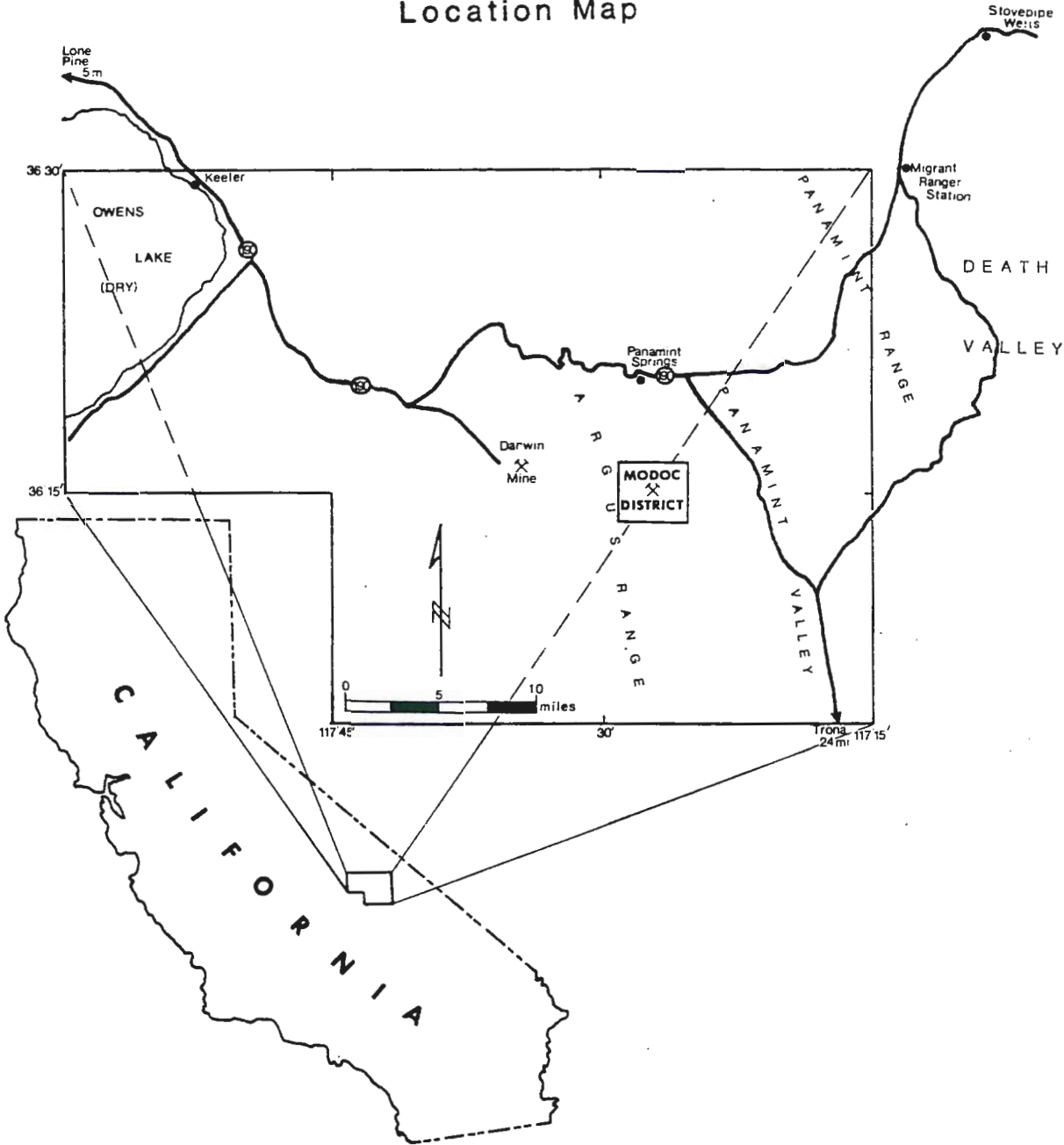


Figure 1. Location map of the study area.

## METHODS OF STUDY

Field work consisting of surface and underground mapping, and sampling, was carried out between May 30 and July 16, 1982. Surface geological mapping and sampling was conducted by pace and compass traverse, on a topographic base, at a scale of one inch to 500 feet (1:6000). The map area has dimensions of approximately 3 x 5 km, roughly 15 km<sup>2</sup> in area. In addition to surface mapping, approximately 1700 meters of underground mapping was completed using tape and compass methods, at a scale of one inch to 50 feet (1:600). The underground mapping was concentrated within the Modoc Mine workings.

Ninety three thin sections were studied to determine lithologies, textural relationships, extent of alteration, and the degree of metamorphism. Estimates of modal mineralogy and textural relationships of representative samples are listed in Appendix A.

Ten polished sections were studied for ore mineralogy, textures, and paragenesis. Modal mineralogy of all samples is listed in Appendix B.

One hundred and twenty-five samples of metamorphic carbonate rocks were assayed for their trace Au, Ag, Pb, Cu, Zn, Mn, content by the Shasta Analytical Geochemistry Laboratory of Redding, California. These analyses are listed in Appendix C. Only some samples were

assayed for Cu, Zn, and Mn.

Ten intrusive rock samples were analyzed by X-ray fluorescence, using an automated Phillips spectrophotometer unit with a computer, for whole rock and trace elements. X-ray fluorescence work was carried out at Michigan Technological University under the supervision of Dr. William Rose. These results are listed in Appendix D.

Also, heels of almost all of the thin sections were stained using either the cobaltinitrite stain for potassium (Chayes, 1952; Rosenblum, 1956; Bailey, 1960) or the alizarine red S stain for calcite (Friedman, 1959).

## PREVIOUS WORK

Early mining activity (1882 to 1896) in the Modoc District is described within numerous reports of the California State Mineralogist. Later mining activity is described in reports on Inyo County by the California Division of Mines and Geology; these include Waring and Hugvenin (1919), Tucker and Sampson (1938), Norman and Stewart (1951), and Goodwin (1957). Generally, these are limited and deal mainly with mine activity.

The first major contribution to the geology of the Modoc District was by Hopper (1947), who mapped a strip, from the Sierra Nevada to Death Valley, which covered the northern portion of the district. Hall and Stephens (1963), of the U.S.G.S., mapped the Modoc District at a scale of 1:20,000 and described the general geology, structure and mineral deposits of the area. Contributions are numerous, with regard to age relationships of the rock units within the area, and include the following. Oliver\* collected four samples of Amphipora sp. from the Modoc and Minnietta Mine areas, in the Lost Burro Formation, and concluded that the age is most likely middle or later Devonian. Sando\* studied coral assemblages from the Tin Mountain Formation and found them to be similar to that of the middle and upper Lodgepole limestone, dating the unit as early Mississippian in age. McAllister (1952) reported a Mississippian age for the

\* Written communication to Hall and Stephens (1963)

Perdido Formation, based on fossil evidence in the Quartz Spring area. Hall and MacKevett (1958) suggested that the Lee Flat limestone is Mississippian and Pennsylvanian on the basis of stratigraphic position. Douglass\* reported on a collection of fusulines which suggest an age of middle Pennsylvanian for the Keeler Canyon Formation; whereas, Wolfcamp\* stated that the characteristic fusulinid is Triticites and dates the formation as early Permian. Duncan\*, on the other hand, collected bryozoans from the upper portion of the formation and found them to be Rhomboporella, which ranges in age from lower to middle Pennsylvanian into the Permian. Stern and Thomas\* dated two intrusions of biotite-hornblende-quartz monzonite in the Argus Range by lead-alpha and potassium-argon methods, and found them to be 180 million years old.

Between 1957 and 1980 there were many consulting geologists who worked for various companies in the district. Most were concerned with feasibility aspects of reopening the district. King (1957), of King and King Mining Engineers, produced a four page memorandum on the Minnietta Mine, which included descriptions of property holdings, economic geology, and a proposed exploration program. Baker (1963) did work at the Defense Mine, mapping the underground workings at 1:600 scale, and produced a report on stratigraphy, structure, mineralization, and new ore possibilities. He concluded that the ore mineralization was controlled by flat-lying structures which he

\* Written communication to Hall and Stephens (1963).



called "flat structures." These flat structures are probably tension fractures developed during the time of faulting, to relieve stresses between two major northwest trending faults within the mine. Baker proposed an intersection of a fault system and the flat structure in the intermediate level, as a favorable exploration target. He also recommended that the mine be abandoned if the work did not produce significant new ore bodies. Chapman (1980) was hired by Lacana Mining, Inc. to examine the district to determine if low to moderate grade silver mineralization existed near the old Modoc Mine. He concluded that detailed geologic mapping, coupled with exploration drilling, might prove quite successful.

#### REGIONAL GEOLOGY

The region is underlain by a 450-meter-thick sequence of metamorphic and sedimentary rocks of Precambrian (?) to Permian age, which are intruded by quartz monzonite plutons of Jurassic age and andesite porphyry dikes of Cretaceous (?) age. Late Cenozoic volcanic rocks and sedimentary deposits unconformably overlie the older rocks (Hall and Stephens, 1963) (Figure 2).

Late Precambrian (?) metamorphic rocks, which include micaceous and carbonate-rich quartzite, mica schist, biotite-hornblende gneiss, and dolomite, are limited to three small exposures in the Panamint Range and Panamint Valley. Paleozoic strata vary in age from middle (?) Cambrian to Permian and form a sequence approximately 4300 meters

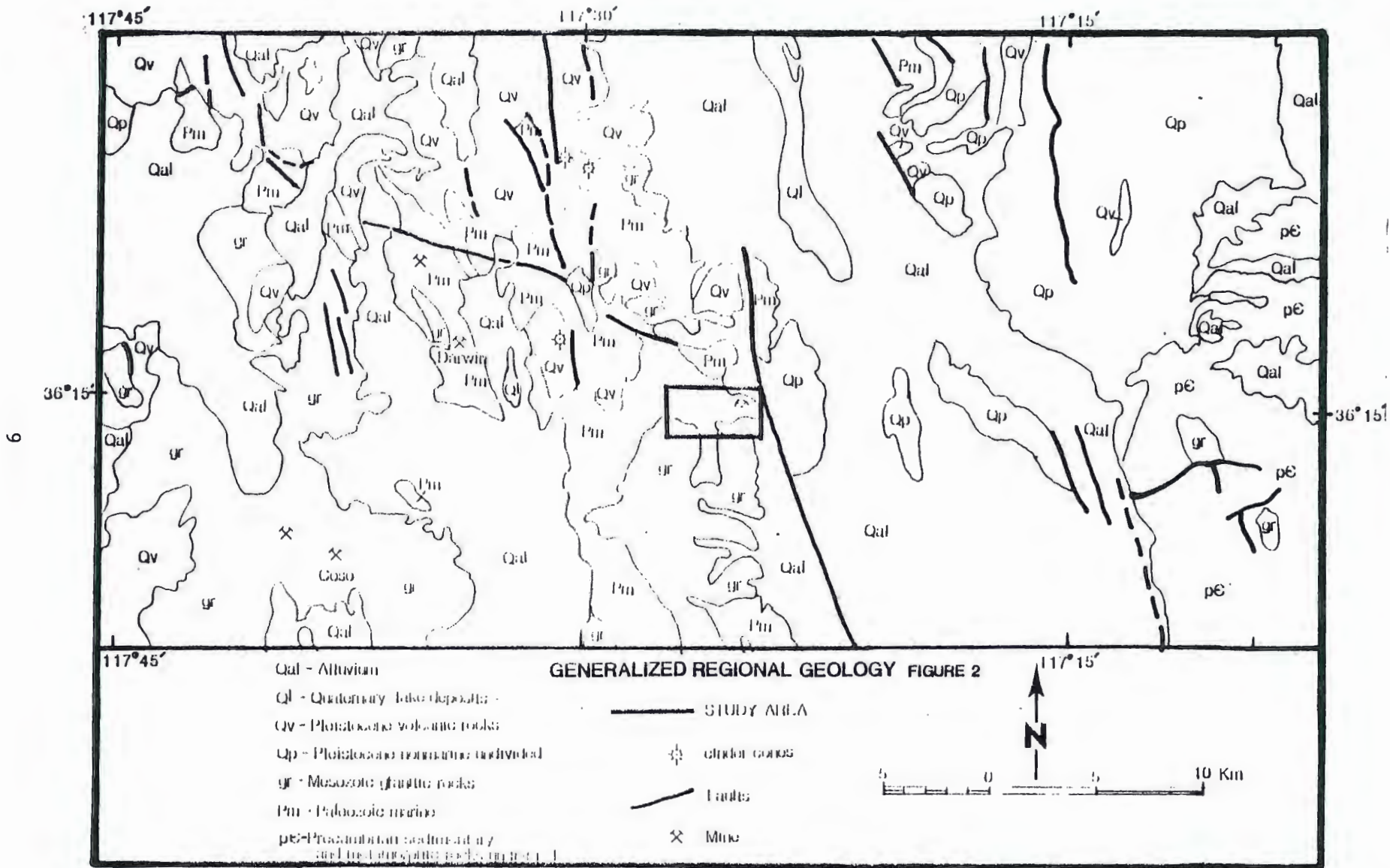


Figure 2. Regional geology map (Jennings, 1958).

thick. Silurian and older Paleozoic rocks are exposed only in the Panamint Range; they consist mainly of dolomite but include lesser amounts of quartzite, limestone and shale. Devonian and younger Paleozoic rocks are exposed both in the Panamint and Argus Ranges and consist predominantly of limestone, marble, and silty limestone (Hall and Stephens, 1963).

Quartz monzonite plutons of Jurassic age intrude the Precambrian (?) and Paleozoic strata in both the Panamint and Argus Ranges. All known producing mineral deposits are within 1.5 miles of these intrusions. A swarm of altered andesite porphyry dikes of Cretaceous (?) age intrudes the Paleozoic rock and, locally, the quartz monzonite in the Argus Range south and southwest of Panamint Springs (Figure 3). Late Cenozoic deposits cover most of Panamint Valley and the Panamint Range south of State Highway 190 (Figure 2).

Three periods of deformation are recognized (Hopper, 1947). The earliest formed broad open folds and major thrust and strike-slip faults due to east-west compressional stresses during the early Mesozoic. The folds trend north to northwest in the Argus and Panamint Ranges. The second period of deformation was due to the forcible intrusion of quartz monzonite plutons of Jurassic age, which deformed both the broad folds and the thrust faults. This was followed by a long period of erosion until the late Cenozoic when extensive regional warps and accompanying strike-slip and normal faults formed the present basin and range topography (Hopper, 1947).

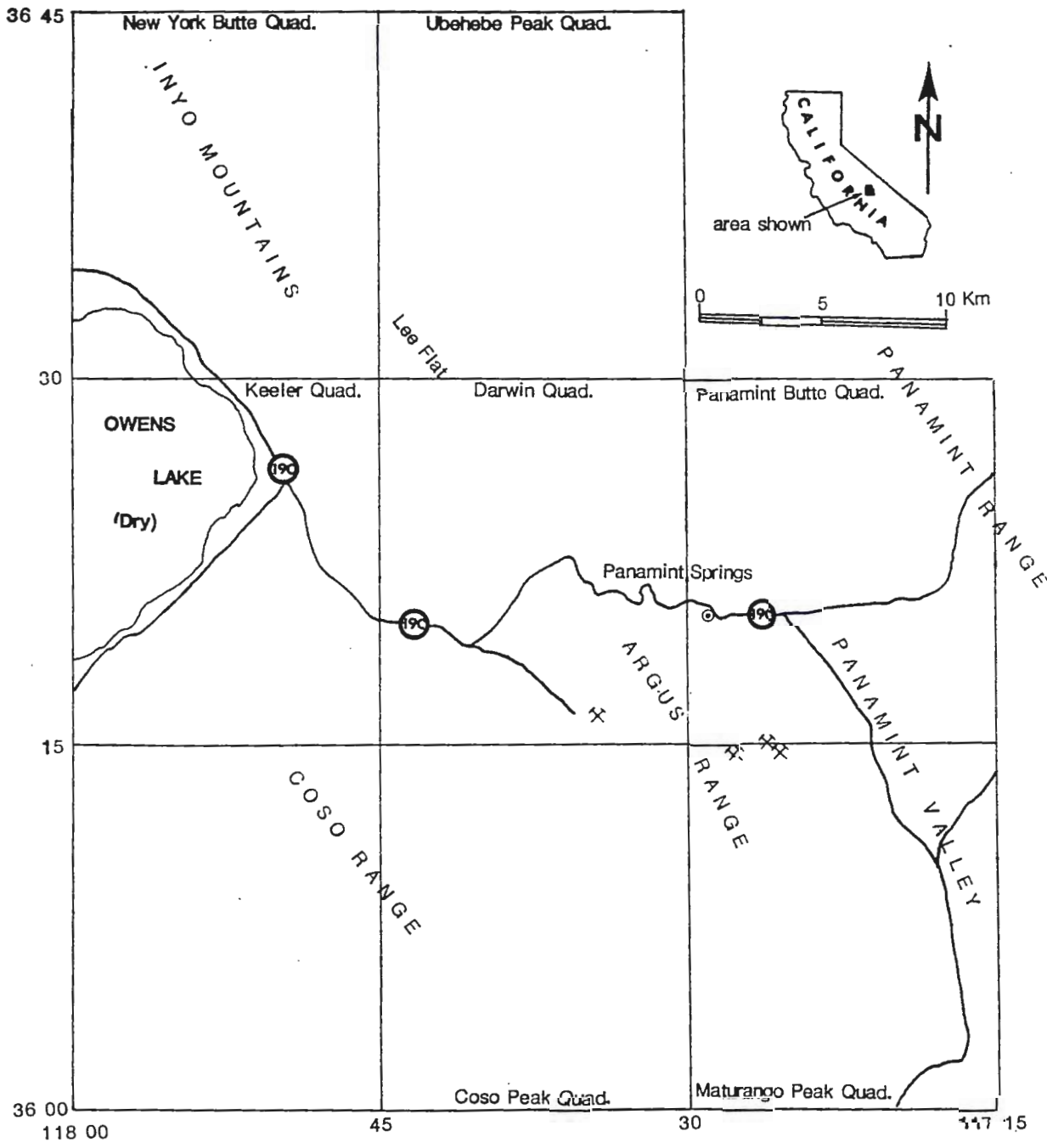


Figure 3. Index map showing quadrangle locations.

## LITHOLOGY AND STRATIGRAPHY

### PALEOZOIC ROCKS

#### GENERAL FEATURES

The Paleozoic stratigraphic section in the Modoc District consists predominantly of carbonate rocks which are similar to formations in the eastern part of the Great Basin (Hall and MacKevett, 1958). Devonian rocks are composed of dolomite, limestone, and quartzite; whereas, Mississippian and younger Paleozoic rocks consist mainly of limestones. No volcanic or phosphatic material, and only minor carbonaceous material, was recognized in the Paleozoic rocks. The minor amounts of carbonaceous material, usually less than 1%, is pervasively distributed throughout the matrix of some beds, and colors the fresh limestone gray to black. Most of the formations are well exposed and some units form bold, cliff-like outcrops. A stratigraphic section is given in Figure 4.

The Paleozoic section in the district has an apparent aggregate thickness greater than 1600 meters (Figure 4); folding and faulting preclude a more accurate appraisal of the thickness. Formation names used by McAllister (1952, 1955) for the Ubehebe Peak Quadrangle and Quartz Spring areas (Figure 3) are generally applicable to the Paleozoic rocks of the study area and have been utilized. Lee Flat limestone, a time stratigraphic equivalent of part of McAllister's

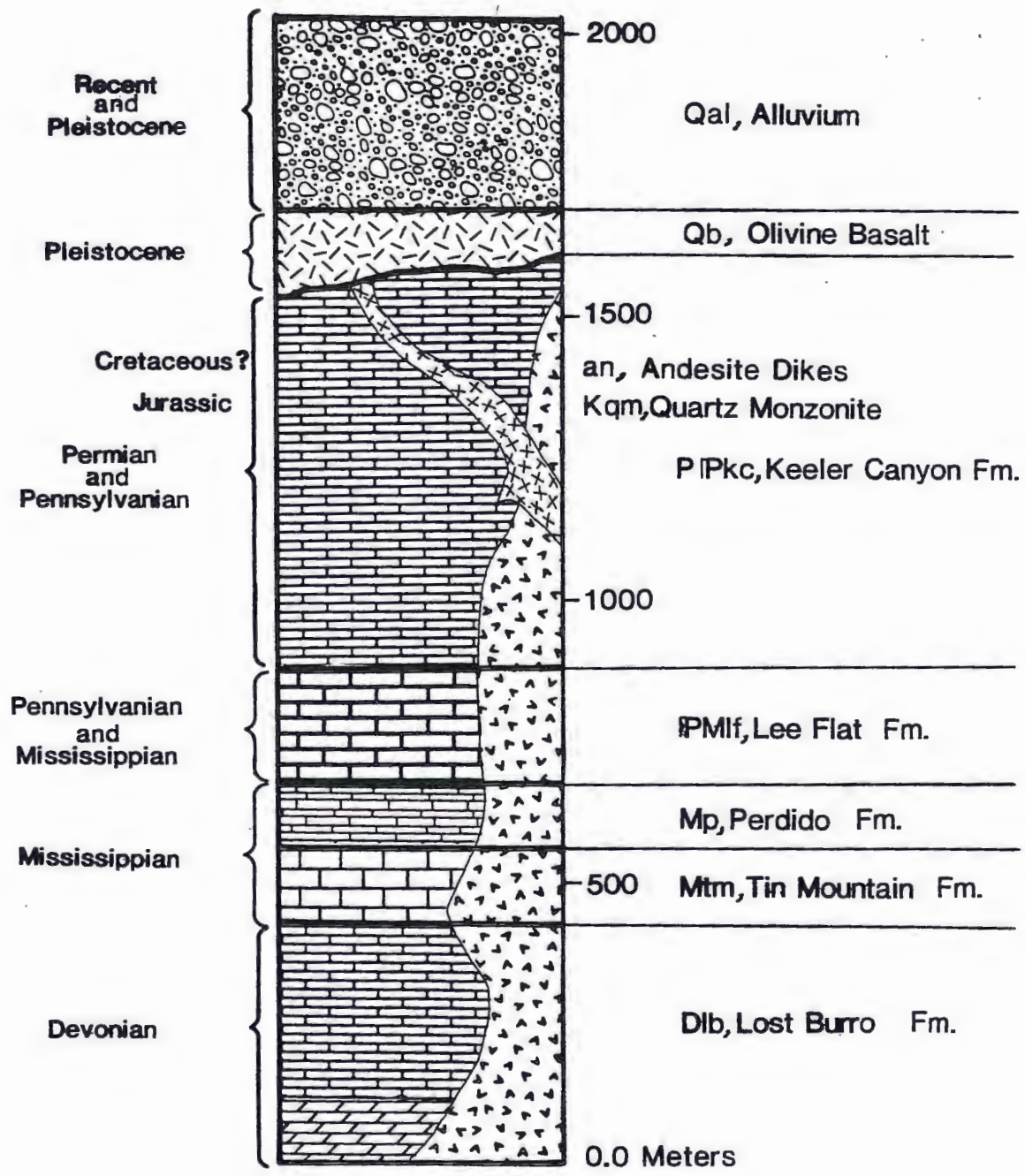


Figure 4. Stratigraphic section of the Modoc District.

Perdido Formation and the Rest Spring shale, was described as a new formation by Hall and MacKevett (1958). Nomenclature used by Merriam and Hall (1957) has been adopted for the Pennsylvanian and Permian Formations. Most of the formations are fossiliferous, though large barren stratigraphic thicknesses occur. The paleontologic record is best documented by an abundant Pennsylvanian and Permian fusulinid fauna, and by corals and brachiopods in the Tin Mountain and Lost Burro Formations of Mississippian and Devonian ages, respectively (McAllister, 1952; Merriam and Hall, 1957).

#### DEVONIAN SYSTEM

##### Lost Burro Formation (unit D1b , Plate 1)

The Lost Burro Formation is middle to late Devonian in age, making it the oldest rock type in the Modoc District (Oliver). The Lost Burro is the dominant rock type at Lookout Mountain, which is situated between the Modoc and Minnietta Mines (Plate 1, Figure 5). The formation's precise stratigraphic thickness is not known due to a large amount of folding and faulting; however, from the present work it is believed to be approximately 430 meters thick. Exposures within the area are composed almost entirely of limestone, in large part, recrystallized to marble. Thin dolomite beds and quartzite lenses were occasionally observed. The limestone is bluish gray in color, thinly to thickly bedded (10 cm to 10 m), with a grain size ranging from 0.5 to 1.5 mm. Where the limestone is recrystallized to

marble it is much coarser grained (1 to 4 mm in diameter) and has a distinct buff color. In many locations the dark limestone and lighter marble beds alternate, giving the Lost Burro Formation a striped appearance (Figure 6). Dolomite, where present, is light brown in color with a distinct sugary texture. The dolomite forms distinct beds (3 to 100 cm thick) and also occurs as swirled patches which cross-cut bedding.

In thin section, the limestone is composed of fine- to medium-grained (0.5 to 1.5 mm in diameter) calcite with minor amounts of fine (0.1 to 0.5 mm in diameter), interstitial tremolite, quartz, and hematite (Figure 7, Table III). The marble consists almost entirely of an interlocking mosaic of calcite (1 to 4 mm in diameter), with minor quantities (< 2%) of tremolite, diopside, quartz, and hematite (Table III, Appendix A). A few samples also contained a white mica (muscovite?) and a highly calcic scapolite (meionite) (Figure 8). The dolomite is noticeably darker, with angular grain boundaries which range from 0.5 to 3 mm in size. The quartzite lenses exhibit 0.5 to 1.5 mm recrystallized quartz grains, which make up 90 to 95% of the rock. Subordinate minerals include tremolite, diopside and calcite.





Figure 5. East side of Lookout Mountain, showing the Lost Burro Formation.



Figure 6. Lost Burro Formation, exhibiting alternating dark limestone and lighter marble beds. Hammer handle is 20 cm long.

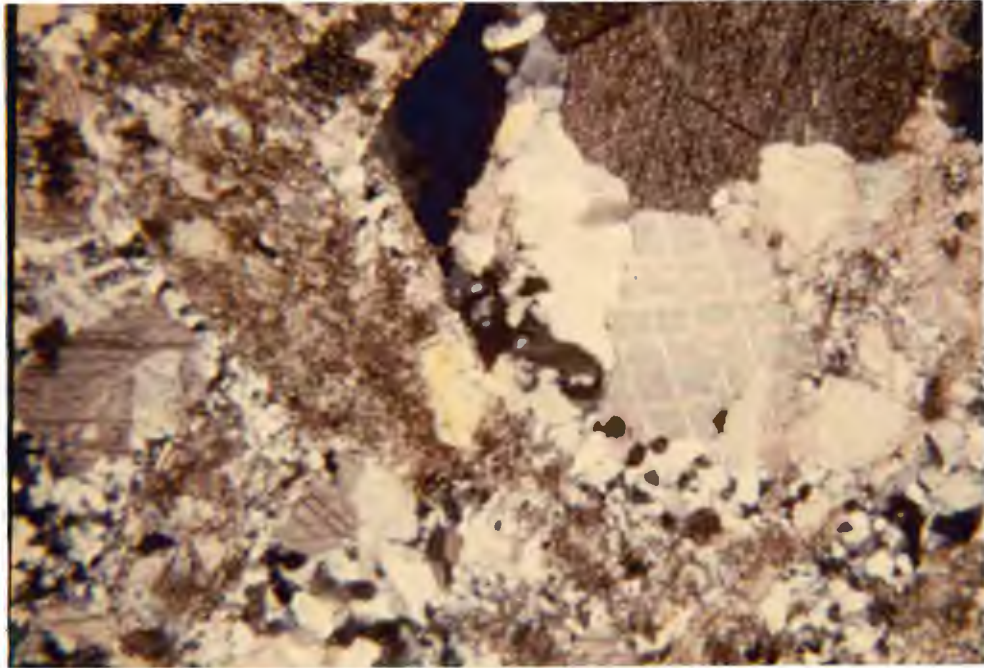


Figure 7. Photomicrograph of Lost Burro limestone showing dark prismatic tremolite grains in a matrix of equigranular calcite. Plane polarized light. Field of view: 5.3 x 3.8 mm.

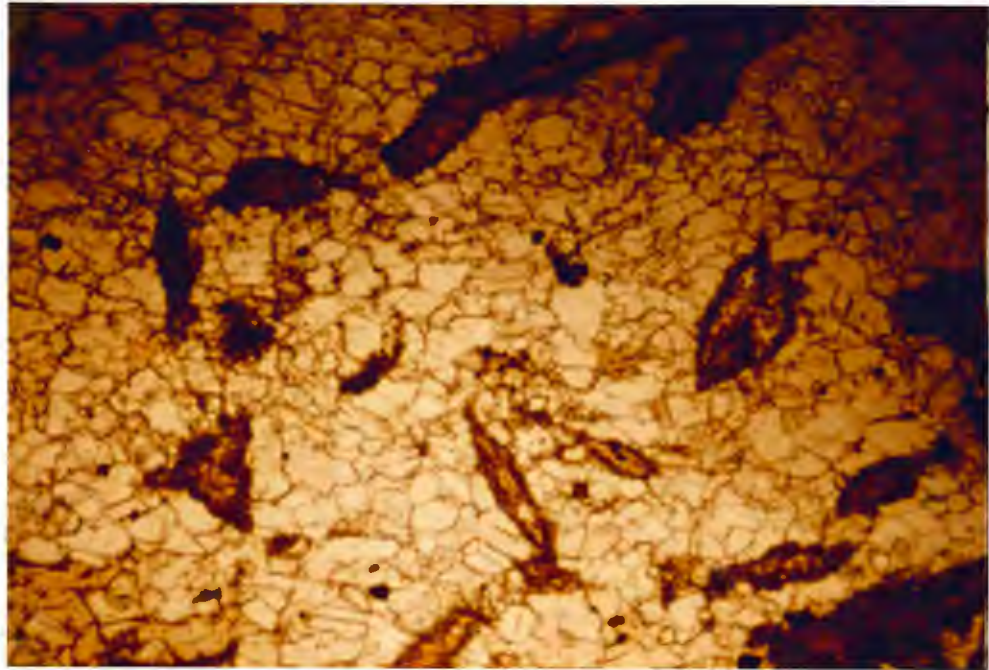


Figure 8. Photomicrograph of Lost Burro marble with cross-cutting quartz veins. Crossed polars. Field of view: 5.3 x 3.8 mm.

## MISSISSIPPIAN SYSTEM

### Tin Mountain Formation (unit Mtm , Plate 1)

The Tin Mountain Formation, which conformably overlies the Lost Burro Formation, was named by McAllister (1952) from exposures at the northernmost peak in the Panamint Range (Figure 3). Several collections of fossils from the Santa Rosa Hills area substantiate an early Mississippian age for the formation (Sando). The Tin Mountain limestone is 150 meters thick at its type location in the Quartz Spring area (McAllister, 1952) and is 120 meters thick where measured in the Modoc District (Hall and Stephens, 1963).

The Tin Mountain Formation consists predominantly of fine-grained (0.25 to 2 mm in diameter), dark gray limestone. Chert lenses and nodules are common throughout the formation, but bedded chert is absent (Figure 9). Much of the limestone is bleached and recrystallized to marble and is difficult to distinguish from the marble of the Lost Burro Formation.

Under the microscope, the marble is composed dominantly of interlocking grains of sparry calcite (2 to 3 mm in diameter), with trace amounts of magnetite and/or hematite (< 0.1 mm in diameter). In most of the sections, calcite exhibits deformed twins, and cleavage is bent and wavy (Figure 10). These textures define a distinct foliation which is parallel to bedding. The gray limestone



Figure 9. Tin Mountain Formation, showing chert nodules in limestone. Hammer handle is 20 cm long.

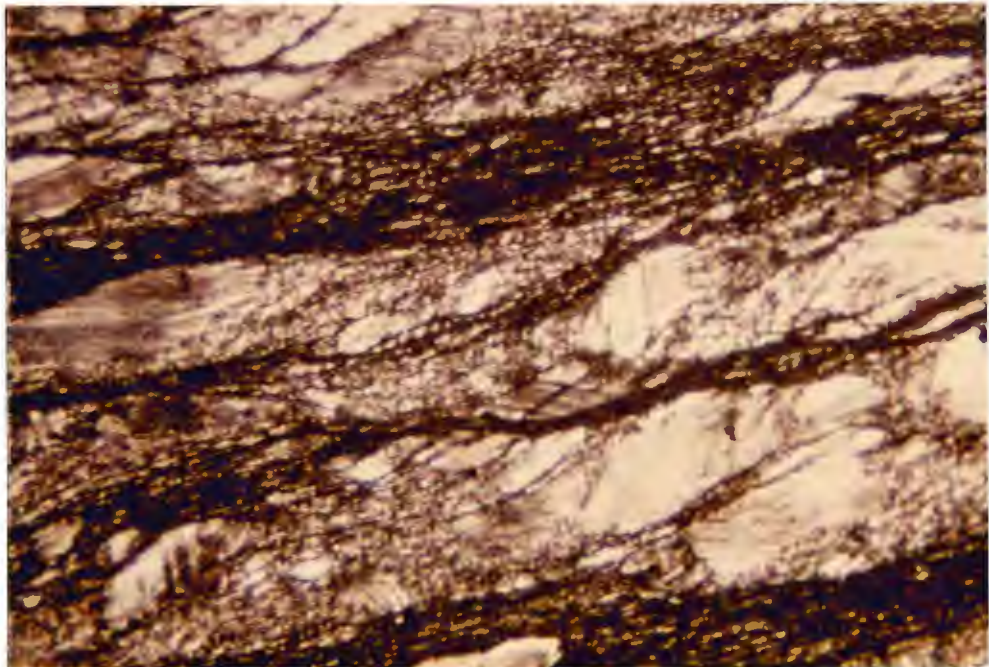


Figure 10. Photomicrograph showing shear foliation in the Tin Mountain Formation. Note the wavy cleavage in the larger calcite grains. Plane polarized light. Field of view: 5.3 x 3.8 mm.

is composed of a mosaic of fine (0.5 to 1 mm in diameter) calcite grains with abundant fossil forms which are replaced by coarse, sparry calcite and recrystallized quartz. In locations where the Tin Mountain Formation is in direct contact with the quartz monzonite intrusive, a distinct contact metamorphic aureole (1 to 5 m wide) has developed. The mineralogy of the rocks within this aureole is similar to that which is described for pyroxene-hornfels facies metamorphism (Turner, 1958). Samples from this zone are composed of equal amounts of poikiloblastic diopside (0.5 to 3 mm in diameter) and idocrase (1 to 6 mm in diameter), with minor amounts of grossular garnet and sparry calcite (Table IV). Trace quantities of periclase (altered to brucite) and wollastonite also occur.

Perdido Formation (unit Mp , Plate 1)

Exposures of the Perdido Formation (named by McAllister in 1952) occur in the Modoc District as a thin band around the nose of a north-plunging anticline (Plate 1). The formation is a cliff-forming unit approximately 110 meters thick; this, and its dark brown weathered color, make it a conspicuous horizon marker. The unit consists of thinly bedded, fine-grained, gray limestone with abundant thin (< 10 cm), brown-weathering beds and veinlets of chert (Figure 11). Near intrusive contacts these thin-bedded rocks are commonly contorted and altered to calc-silicate minerals.

Silty micrite beds, 5 to 20 cm thick, are the dominant component of

the formation where it is not metamorphosed. In thin section the micrite consists of 60 to 85% calcite grains, which range from 0.05 to 0.1 mm in diameter, and 15 to 40% chert (Table V). Chert beds are composed of an interlocking mosaic of quartz grains, 0.1 to 0.5 mm in diameter.

The majority of the Perdido Formation is metamorphosed to pyroxene-hornfels facies close to intrusive contacts (Plate 1), and to hornblende-hornfels facies away from contacts. Rocks in the pyroxene-hornfels facies can be subdivided into two distinct mineral assemblages: a) wollastonite, diopside, grossular, and calcite, and b) idocrase, diopside, grossular and calcite (Table V). Hornblende-hornfels facies rocks are composed of calcite, tremolite, diopside, and quartz (Table V). The chert beds within these metamorphosed rocks are recrystallized to coarser quartz grains. Few fossils were observed, except for crinoid columnals which sometimes form coarse clastic beds. On the basis of stratigraphic position, the Perdido Formation is younger than the Tin Mountain Formation and older than the basal part of the Lee Flat limestone. On the basis of fossil evidence in the Quartz Spring area, McAllister (1952) reported a Mississippian age for the Perdido Formation.



Figure 11. Perdido Formation with alternating chert and silty micrite beds. Note boudined chert beds. Hammer handle is 20 cm long.

## MISSISSIPPIAN AND PENNSYLVANIAN SYSTEM

### Lee Flat Limestone (unit IPMLf, Plate 1)

The Lee Flat limestone was named for exposures on the southwest side of Lee Flat (Figure 3) (Hall and MacKevett, 1958). White marble of the Lee Flat limestone crops out around the upturned edge of the north-plunging anticline in the Modoc District (Plate 1). The formation is approximately 200 meters thick. Crinoidal fragments are the only fossils found in the formation (Hall and MacKevett, 1958); due to this poor fossil record, the age of the formation is based on stratigraphic position. It is considered to be Mississippian and Pennsylvanian in age.

The Lee Flat limestone consists entirely of clean, white to very light gray marble (or sparite) with an average grain size of 2 to 4 mm. Beds are commonly less than 30 cm thick, but the uniform white color gives the formation a more massive appearance (Figure 12). Partial dolomitization of the marble is common near faults.

Thin sections show that the Lee Flat limestone has been extremely recrystallized and now consists chiefly of calcite grains (2 to 7 mm in diameter) which have very sharp grain boundaries. Quartz, hematite, and limonite make up about 1 to 2% of most sections (Table VI). An example of the recrystallized Lee Flat limestone can be seen in Figure 13.





Figure 12. Massive white marble of the Lee Flat Formation. Hammer handle is 20 cm long.

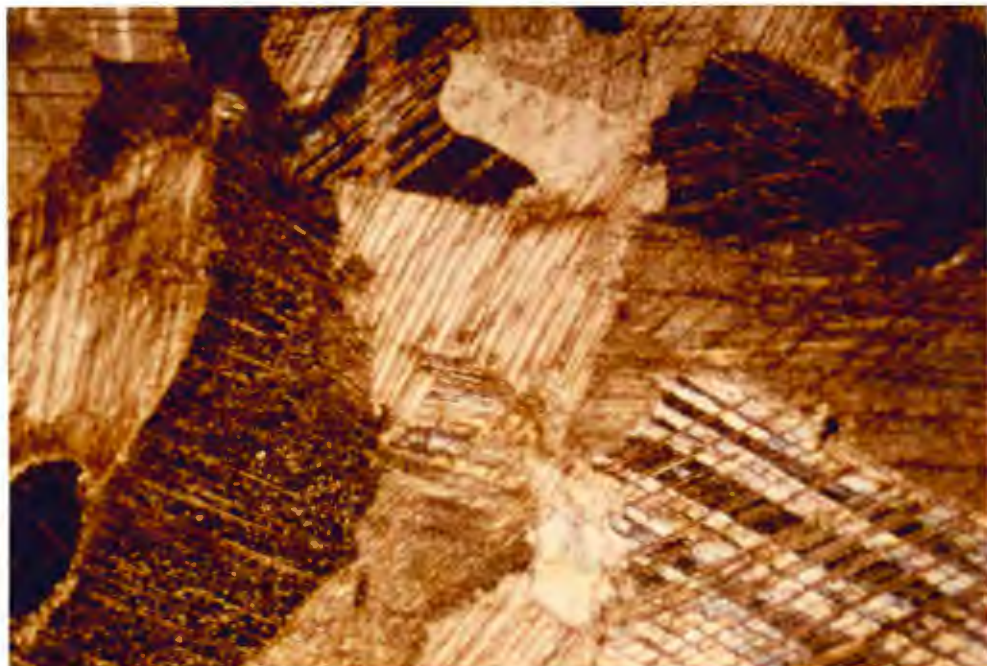


Figure 13. Photomicrograph of sparry calcite grains of the Lee Flat Formation. Crossed polars. Field of view: 5.3 x 3.8 mm.

## PENNSYLVANIAN SYSTEM

### Lower Unit Keeler Canyon Formation (unit P [Pkc, Plate 1)

The name Keeler Canyon Formation was proposed by Merriam and Hall (1957) for a thick sequence of rocks east of the Estelle Tunnel Portal at the head of Keeler Canyon (Figure 3). The formation is divided into two units: 1) a lower unit (700 meters thick) which is composed mainly of bluish gray limestone and limestone pebble conglomerate, and 2) an upper unit (540 meters thick) composed largely of pinkish shales with minor shaly limestones. Fusulinids were found within 30 meters of the base of the formation. Douglass reported on a collection from this zone and suggested a middle Pennsylvanian age.

Only the basal 150 meters of the lower unit is exposed within the map area, thus it will be the only portion described. The formation consists of thinly (3 to 10 cm) bedded, dark gray limestone with intercalated gray limestone-pebble conglomerate beds (0.3 to 1.5 m thick). These beds contain small fusulinids, about 2 mm long, and minor chert nodules. Spheroidal black chert nodules, about 1 to 5 cm in diameter, are common in the thicker limestone beds near the base of the unit (Figure 14). This zone is a reliable stratigraphic marker and is referred to as the "Golfball" horizon by Merriam and Hall (1957).

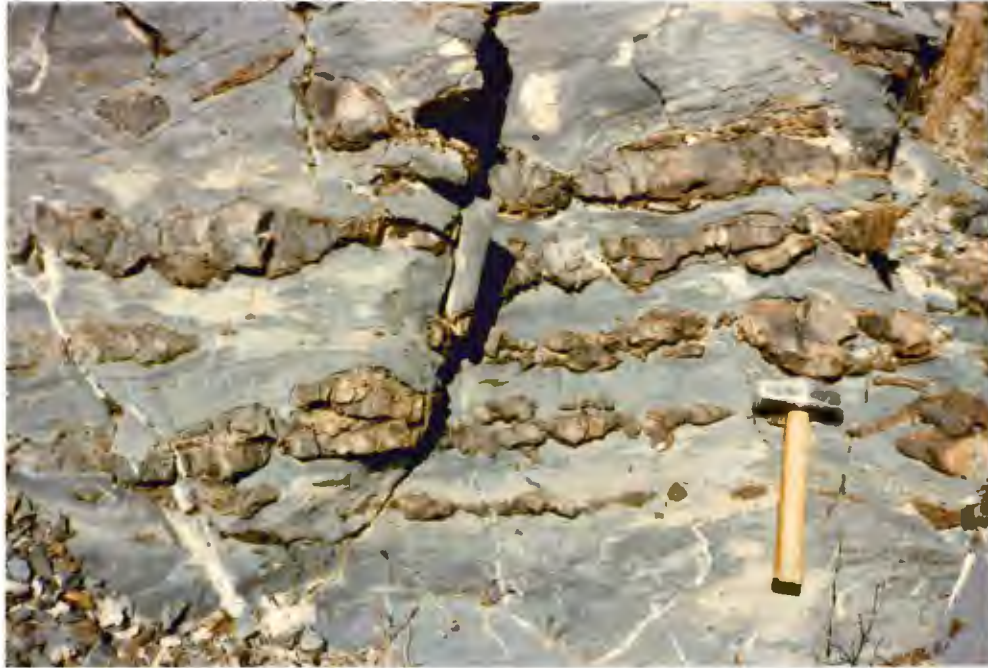


Figure 14. Keeler Canyon Formation with chert nodules, on the edge of the "Golfball" horizon. Hammer handle is 20 cm long.

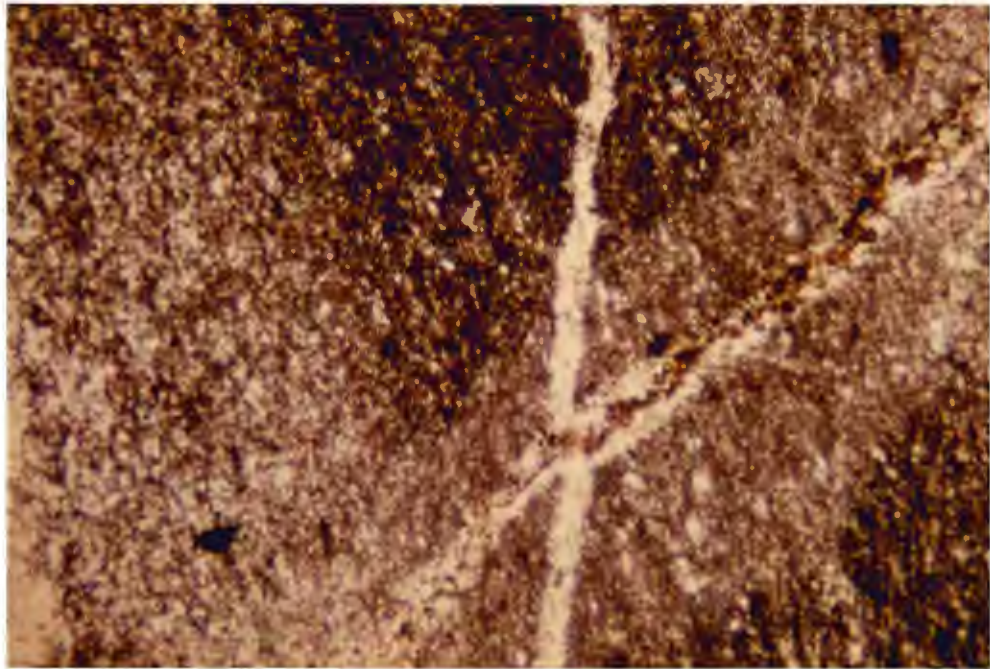


Figure 15. Photomicrograph of silty micrite with cross-cutting, sparry calcite veins (Keeler Canyon Formation). Crossed polars. Field of view: 5.3 x 3.8 mm.

Thin section studies show that the thinly bedded, dark gray limestone is a silty micrite. This micrite is composed of equal amounts of rounded calcite grains (0.02 to 0.5 mm in diameter), fine (0.05 to 0.1 mm in diameter) quartz, and hematite (4 to 5%) (Table VII). Chert beds and nodules within the micrite are fractured, and are commonly filled with secondary sparry calcite (Figure 15). Under the microscope the limestone pebble conglomerate consists of fusulinid and crinoidal fragments which are replaced by sparry calcite, quartz, and hematite.

#### MESOZOIC ROCKS

##### Biotite-Hornblende-Quartz Monzonite (unit Kqm, Plate 1)

A biotite-hornblende-quartz monzonite pluton crops out in the south and southwestern portions of the Modoc District (Plate 1). This intrusion has been dated by lead-alpha and potassium-argon methods; both give an age of 180 million years (Stern and Thomas).

The quartz monzonite is a light gray rock that has a speckled appearance produced by disseminated mafic minerals. The texture ranges from equigranular, with an average grain size of 2 to 3 mm, to porphyritic. The porphyritic texture is produced by 10 to 15% phenocrysts of pink potassium feldspar (1.5 cm in diameter), which are set in a finer grained (1 to 3 mm in diameter), light gray

equigranular groundmass.

In thin section the quartz monzonite is composed of potassium feldspar, plagioclase, quartz and more than 5% each of hornblende, chlorite and biotite (Table VIII). Feldspar makes up 54 to 66% of the rock, with plagioclase exceeding the average potassium feldspar content by about 5%. Plagioclase ranges from calcic oligoclase ( $An_{28}$ ) to andesine ( $An_{45}$ ), and commonly shows normal zoning. The approximate compositions for the plagioclase were determined by the Michel-Levy Statistical Method (Heinrich, 1965). The potassium feldspar is orthoclase and is commonly microperthitic. Some feldspar has microcline twinning, particularly the phenocrysts. The quartz content ranges from 10 to 30%, but usually constitutes about 15% of the rock. The quartz occurs as anhedral grains (0.5 to 2 mm in diameter) with many showing undulatory extinction. Mafic minerals compose approximately 20% of the rock; hornblende is generally the most abundant. Accessory minerals include magnetite (2% or greater), apatite, sphene, zircon, epidote, and sericite (all trace to 2%) (Figure 16, Table VIII).

#### Other Intrusive Rocks (Pods or Dikes) (units Ka, Ks, Kg, Plate 1)

Felsic dikes or pods are present within the Modoc District on the outer fringes of the quartz monzonite pluton (Plate 1). These border facies intrusives include syenite and granophyric granite, plus an aplite dike.

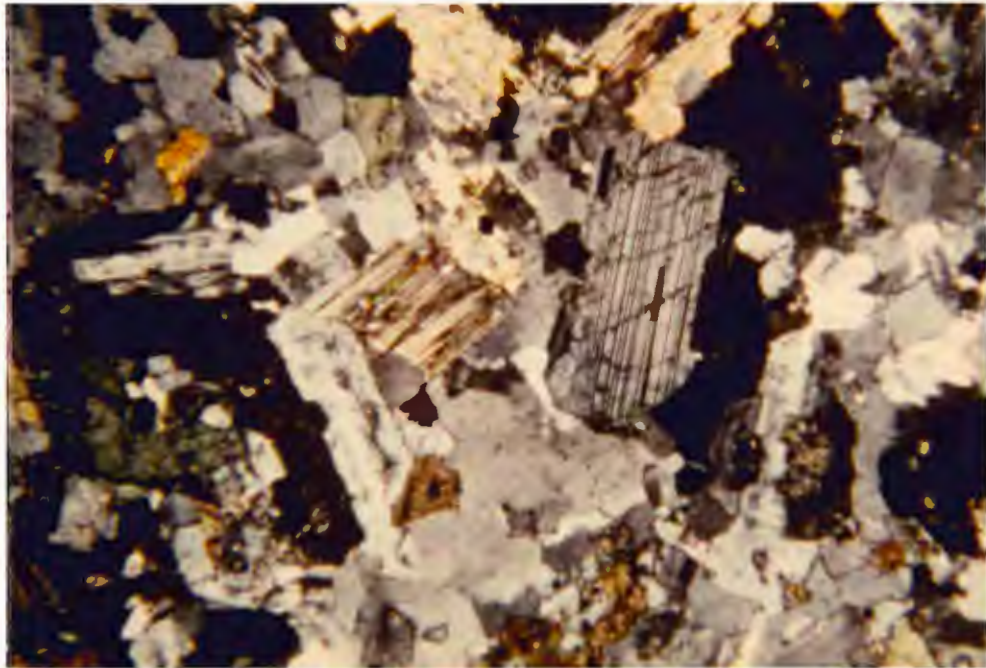


Figure 16. Photomicrograph of biotite-hornblende-quartz monzonite. Note twinned plagioclase, K-feldspar, hornblende, biotite altering to chlorite, sphene and magnetite. Crossed polars. Field of view: 5.3 x 3.8 mm.

A 1.5 meter thick aplite dike, which crops out near the main adit at the Defense Mine (Plate 1), contains equal amounts of aphyric quartz and microcline (2 mm in diameter), with subordinate plagioclase, biotite, and chlorite. Minor accessory apatite and sphene are also present.

A dike at the lower tunnel of the Defense Mine, and exposures to the west of the mine (Plate 1), are composed of perthitic-augite-syenite. This rock consists of 45% alkali feldspar, 39% augite, 9% plagioclase and 2 to 3% apatite and sphene.

Pods or dikes of granophyric granite locally occur at the contact of the Perdido Formation and the quartz monzonite (near the switchback on the road to Lookout Mountain) (Plate 1). The rock is dark gray and coarse-grained (3 to 6 mm in diameter), with white feldspar patches in a darker quartz matrix. Feldspars, which make up 45% of the rock, are microcline and microperthitic orthoclase. Twenty-five percent of the quartz appears as 0.5 mm intergrowths in feldspar with the remaining 20% forming individual grains, 1 to 2 mm in diameter. The only other mineral observed was euhedral sphene, which makes up approximately 1% of the rock.

#### Altered Andesite Porphyry Dikes (unit an, Plate 1)

Altered, fine-grained, porphyritic, greenish-gray dikes of andesitic composition crop out throughout the Modoc District. One prominent

dike, 0.5 km long, cross-cuts quartz monzonite, as well as Paleozoic rocks, in the southern part of the district. Many dikes occur along fault boundaries near the Minnietta Mine (Plate 1, Figure 17). These dikes range from 0.5 to 3 m thick and strike between N 70° W and West, with dips close to vertical. The dikes are greenish-gray on freshly broken surfaces, and weather to various shades of brown. In thin section the andesite porphyry dikes consist of primary skeletal remnants of augite and saussuritized plagioclase phenocrysts set in a fine-grained felty groundmass composed dominantly of elongate, saussuritized plagioclase. The augite and plagioclase phenocrysts average 1 - 2 mm in diameter, and the groundmass plagioclase is 0.2 x 0.03 mm. The rock is altered to epidote, albite, chlorite, and calcite. Quartz and hornblende are less common secondary minerals along with minor amounts of magnetite and apatite (Table X). The dikes cut both the Paleozoic carbonate strata and the Mesozoic intrusion, but are older than the lead-silver deposits. They are considered Cretaceous (?) or early Tertiary (?) in age (Moore and Hopson, 1961).





Figure 17. Altered andesite dikes, within fault zones, cross-cutting the Lost Burro Formation. Width of dikes is approximately 2 - 3 m.

## CENOZOIC ROCKS

### Olivine Basalt (unit Qb, Plate 1)

Basaltic lava flows occur as isolated patches, unconformably capping both Paleozoic rocks and quartz monzonite, near the center of the study area (Plate 1). The basalt flows are reddish gray and massive, with thicknesses ranging from 5 to 15 m. Individual basalt flows commonly have a systematic internal structure. A zone of rubbly material occurs at the base and is 15 to 60 cm thick. Above this basal zone the flow grades upward into massive basalt that contains a few (1 to 2%) stretched vesicles. The massive basalt ranges from a few meters to 10 meters in thickness. The basalt itself is a dark gray, finely porphyritic rock containing phenocrysts of olivine and plagioclase in an aphanitic groundmass. Massive basalt then grades upward into scoriaceous basalt, where 5 to 10% vesicles are common. This grades into scoria at the top of a flow. Flow lineations were observed along the top (?) of one flow (Figure 18).

Under the microscope the basalt phenocrysts are predominantly olivine with small amounts of plagioclase, which are set in a groundmass of plagioclase, olivine, augite and devitrified glass (Table XI). The euhedral to subhedral olivine phenocrysts are 1 to 3 mm in diameter, and are partly to entirely altered to iddingsite. The groundmass has a trachytic texture and is composed of plagioclase ( $An_{57-60}$ ) laths (0.1 to 0.3 mm long), subhedral olivine and augite grains

(0.2 mm in diameter), and devitrified glass. Magnetite and biotite each constitute about 2% of the groundmass (Figure 19).

The age of the olivine basalt is believed to be early Pleistocene or younger (Kelley, 1937; Hopper, 1947).

#### Quartz Porphyry Dike (unit Qp, Plate 1)

A quartz porphyry dike extends across the south-southwestern portion of the study area. This dike cross-cuts all of the rock types within the Modoc District (Plate 1, Figure 20). The dike can be traced along strike for 3.2 km, and ranges in thickness from 5 to 35 m. In outcrop the dike is a light tan to reddish brown, porphyritic rock with phenocrysts of quartz and feldspar (1 to 6 mm diameter), set in an aphanitic groundmass. In thin section, euhedral volcanic quartz crystals (2 to 6 mm in diameter), showing good resorption textures, make up one-half to two-thirds of the phenocrysts. Plagioclase feldspar ( $An_{25-35}$ ) can make up to one-third of the total phenocrysts, with orthoclase and perthitic orthoclase (1 to 2 mm in diameter) accounting for the rest. The felty groundmass consists of a 65 to 75% fine-grained mixture of quartz and feldspar with minor biotite, muscovite, chlorite, zircon, and apatite constituting the rest of the groundmass (Figure 21, Table IX). The age of the dike is unknown; however, the dike cross-cuts the olivine basalt which is thought to be early Pleistocene. From this correlation the dike would be Pleistocene or younger (?).



Figure 18. Olivine basalt lava flow with flow lineations. Hammer handle is 20 cm long.

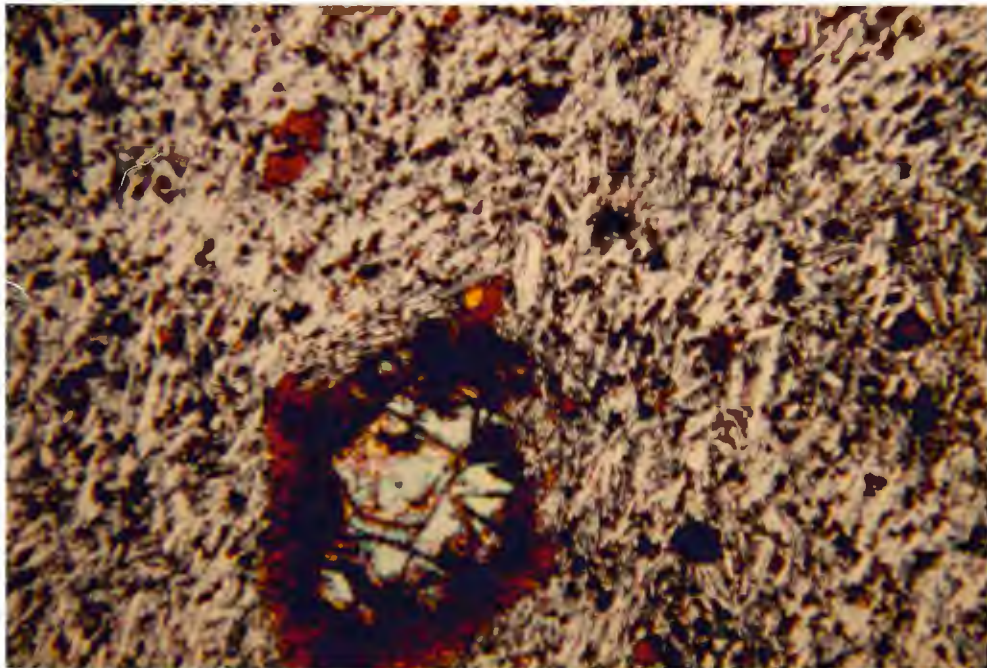


Figure 19. Photomicrograph of olivine basalt flow; olivine phenocrysts altered to iddingsite in a groundmass of plagioclase, olivine, augite, and magnetite. Crossed polars. Field of view: 5.3 x 3.8 mm.



Figure 20. Quartz porphyry dike cross-cutting the Perdido Formation. Dike is 10 - 20 meters wide. Looking northwest from thin section location #363. (Plate 1)

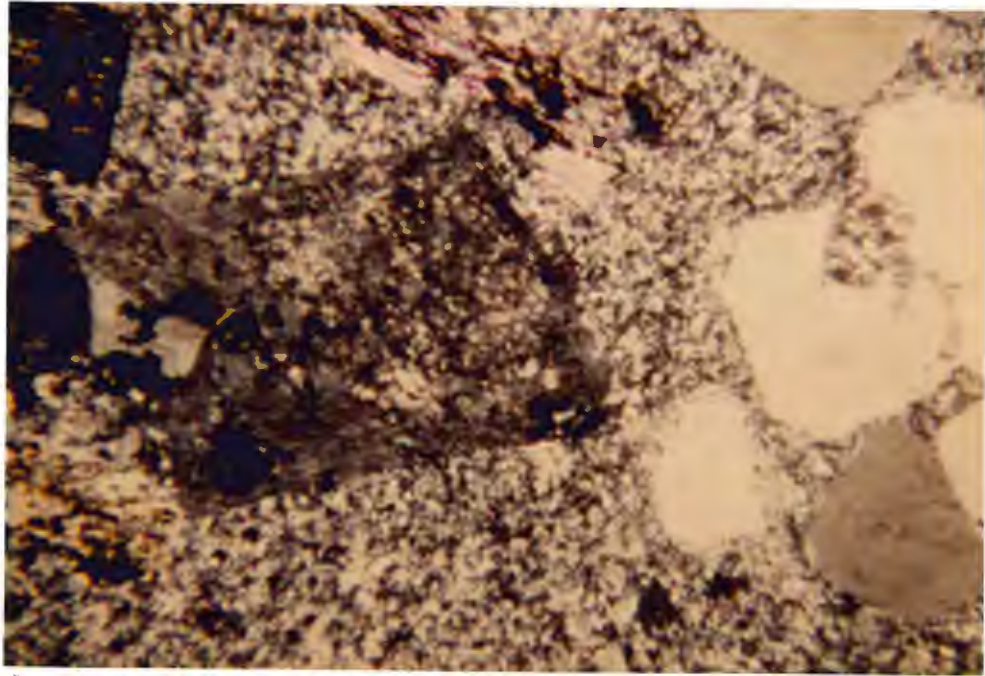


Figure 21. Photomicrograph of K-feldspar, quartz, and muscovite phenocrysts in a felty groundmass in the quartz porphyry dike. Crossed polars. Field of view: 5.3 x 3.8 mm.

## METAMORPHISM AND ALTERATION

### METAMORPHISM AND ALTERATION OF LIMESTONES

#### Introduction

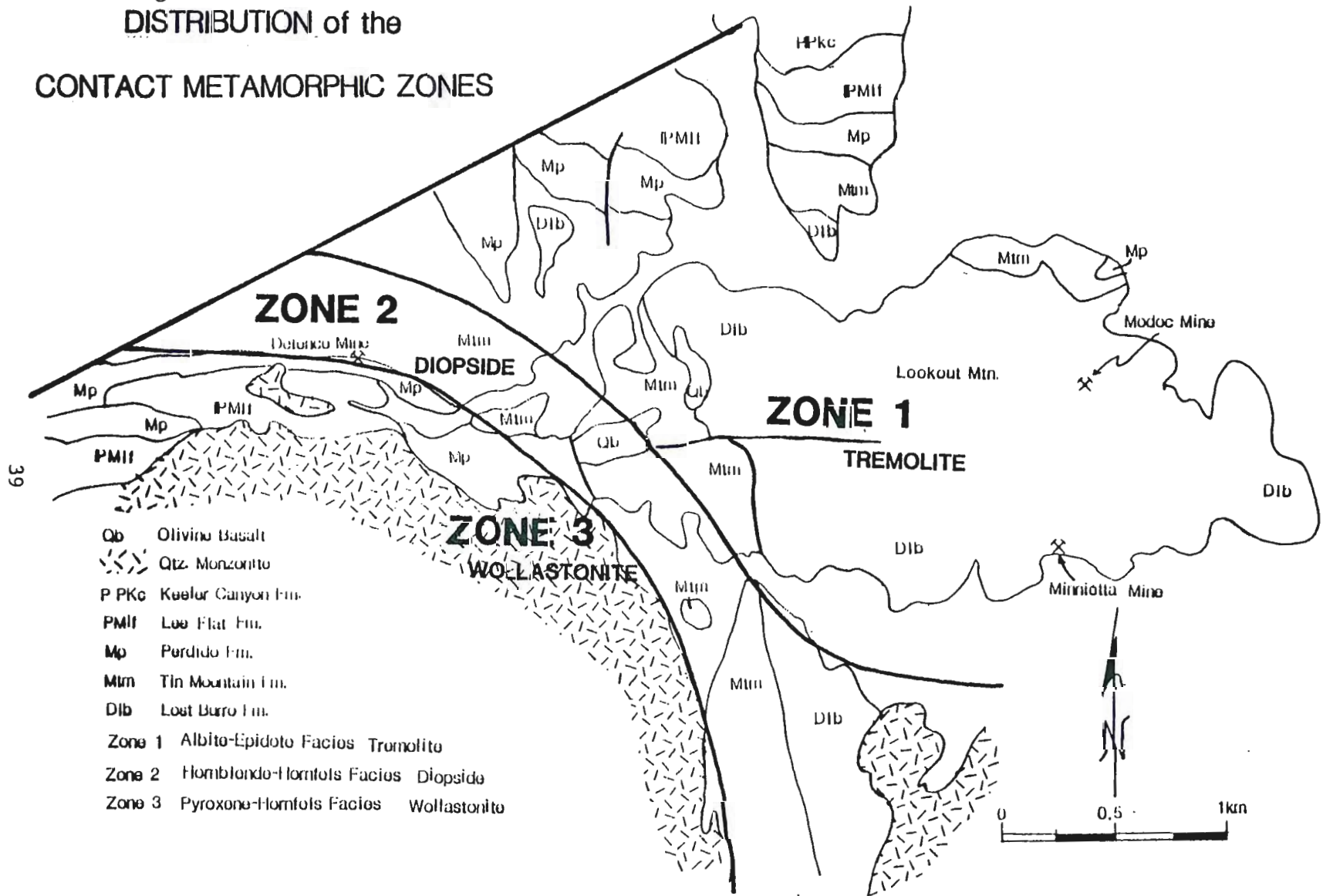
Within the carbonate strata of the Modoc District there are distinct zones of contact metamorphism which developed as an aureole around the quartz monzonite stock (Figure 22). Based on mineral assemblages, the aureole can be divided into three distinct metamorphic zones. Zone 1, which is the outermost zone, is characterized by assemblages which include calcite, dolomite, tremolite, and quartz (Tables III and IV). This assemblage belongs to the albite-epidote-hornfels metamorphic facies (Turner, 1958). Closer to the intrusive contact, within zone 2, diopside becomes a stable phase and these rocks are then characterized by calcite, tremolite, diopside, and quartz + scapolite (Tables III and IV). Assemblages made up of these minerals are found in the hornblende-hornfels metamorphic facies (Turner, 1958). The innermost zone of contact metamorphism reaches the highest grade, and consists of assemblages containing calcite, diopside, wollastonite, idocrase, grossular, and anorthite. These assemblages are characteristic of the pyroxene-hornfels metamorphic facies (Turner, 1958).

Zone 1 (albite-epidote-hornfels facies) is by far the most widespread, being developed from approximately 2.5 km to 700 meters

Figure 22.

**DISTRIBUTION of the**

**CONTACT METAMORPHIC ZONES**



- Qb Olivine Basalt
- Qtz Monzonite
- P PkC Keeler Canyon Fm.
- PMII Lone Flat Fm.
- Mp Perdido Fm.
- Mtn Tin Mountain Fm.
- DIB Lost Burro Fm.
- Zone 1 Albito-Epidoto Facies Tremolite
- Zone 2 Hornblende-Hornfels Facies Diopside
- Zone 3 Pyroxene-Hornfels Facies Wollastonite



away from the intrusive contact. Zone 2 (hornblende-hornfels facies) is formed from approximately 700 to 30 meters away from the intrusive contact; whereas, zone 3 (pyroxene-hornfels facies) ranges from 30 meters away, up to the contact itself (Figure 22).

Though the mineralogical differences between the metamorphic zones are very apparent as distance from the stock increases, variation in original lithologic composition also contributes to the variation in mineralogies seen. The relatively pure Lost Burro and Tin Mountain Formations are, in part, bleached and recrystallized to marble, and in part, altered to a variety of calc-silicate minerals. The very pristine Lee Flat limestone was completely recrystallized to marble with no formation of calc-silicate minerals. In contrast, the silty and sandy limestones of the Perdido Formation, along with a few beds of the Tin Mountain Formation, were extensively altered to calc-silicate rocks close to the intrusive contact. This lithologic control of metamorphism appears to be a more important factor than distance from the intrusive contact.

#### Formation of Calc-Silicate Minerals - Zones 1 and 2

Along with the recrystallization of the limestones to marble, there was the formation of calc-silicate minerals within specific beds of the Lost Burro, Tin Mountain and Perdido Formations during contact metamorphism. These calc-silicate minerals are noted by zones 1 and 2 in Figure 22. Zone 1, the albite-epidote-hornfels facies zone, was

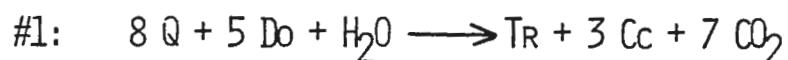
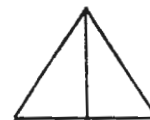
formed where dolomite and quartz reacted to form tremolite and calcite through reaction #1, which is illustrated in Figure 23. The tremolite within these metamorphosed beds makes up from trace to 5% of the limestone (Tables III and IV). Zone 1 is followed inward by zone 2 (hornblende-hornfels facies), which is characterized by the presence of diopside. The formation of diopside probably occurs by the reaction of tremolite + calcite + quartz where the three minerals have been in contact (reaction #2, Figure 23). On the average, the altered rocks within this zone contain 1 to 2 % diopside (Tables III and IV).

#### Alteration to Skarn and Calc-Silicate Hornfels - Zone 3

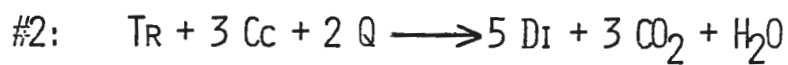
Zone 3 (pyroxene-hornfels facies) has been designated on the basis of the appearance of wollastonite. Wollastonite formed in this high temperature zone through the reaction of calcite and quartz via reaction #3 (Figure 23). In addition, alteration of impure limestone and marble, to calc-silicate hornfels and skarn, is common where the Perdido and Tin Mountain Formations are in direct contact with the quartz monzonite stock. The term calc-silicate hornfels is used herein to describe a densely packed, fine-grained, light-colored rock, which is generally considered to form by the virtually isochemical recrystallization of impure limestone. The term skarn is used to describe a coarse-grained dark-colored rock formed by contact metasomatism of limestone, into which large amounts of Si, Al and Fe have been introduced from the intrusion.

## METAMORPHIC REACTIONS

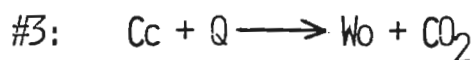
ZONE 1: FORMATION OF TREMOLITE



ZONE 2: FORMATION OF DIOPSIDE



ZONE 3: FORMATION OF WOLLASTONITE



- Do - Dolomite -  $CaMg(CO_3)_2$
- Cc - Calcite -  $CaCO_3$
- Q - Quartz -  $SiO_2$
- TR - Tremolite -  $Ca_2Mg_5Si_8O_{22}(OH)_2$
- DI - Diopside -  $CaMgSi_2O_6$
- Wo - Wollastonite -  $CaSiO_3$

Figure 23. Reactions for the formation of calc-silicate minerals in zones 1-3 (Skippen, 1974).

The Perdido Formation is patchily altered across a 1.5 km by 300 m area around the northern edge of the quartz monzonite stock (Plate 1, Figure 22). The alteration is irregularly developed due to selective metamorphism; impure limestone beds are partly or completely altered to calc-silicates, but pure limestone beds remain unchanged. In the Perdido Formation the metamorphosed rock ranges from a medium-grained (0.5 to 2 mm in diameter), light-colored, calc-silicate rock with minor skarn close to the contact, to a dense, fine-grained (0.02 to 0.05 mm in diameter) white or greenish-gray calc-silicate hornfels away from the contact. The metamorphism is generally more intense, and the rock is coarser grained near the intrusive body, though local exceptions occur due to differences in original bed compositions. Silty limestone beds were readily converted to calc-silicate hornfels and these rocks now consist predominantly of laths of wollastonite (< 0.1 mm in diameter) and diopside (0.1 to 0.5 mm in diameter), with interstitial grossular, calcite, and, in two cases, plagioclase (Figure 24, Table V). Closer to the intrusion, wollastonite forms megacrystalline radial masses (4 to 6 cm in diameter) and large (5 to 10 cm long) crystals. The skarn rock of the Perdido Formation consists predominantly of idocrase and diopside with garnet and minor calcite. The idocrase occurs as large (1 to 4 cm in diameter) euhedral to subhedral prismatic crystals that exhibit color zonation under the microscope (Figure 25, Table V). Garnet, which is widespread throughout both mineral assemblages, increases in grain size and abundance toward the intrusive contact.

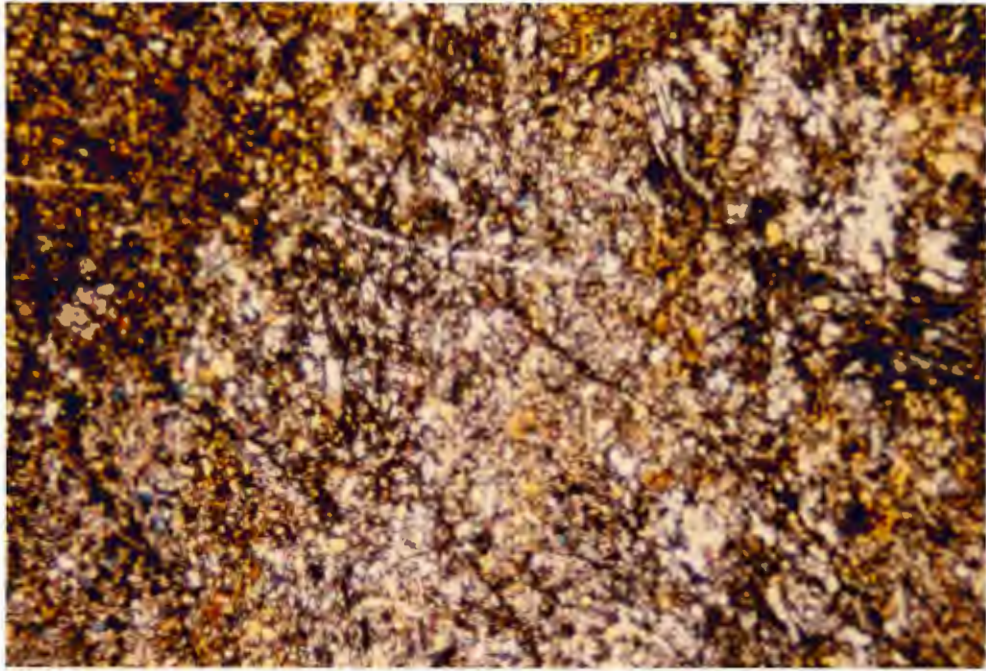


Figure 24. Photomicrograph of hornfels composed of light gray wollastonite laths, highly birefringent blue diopside, calcite and black interstitial garnet. (Perdido Formation). Crossed polars. Field of view: 5.3 x 3.8 mm.

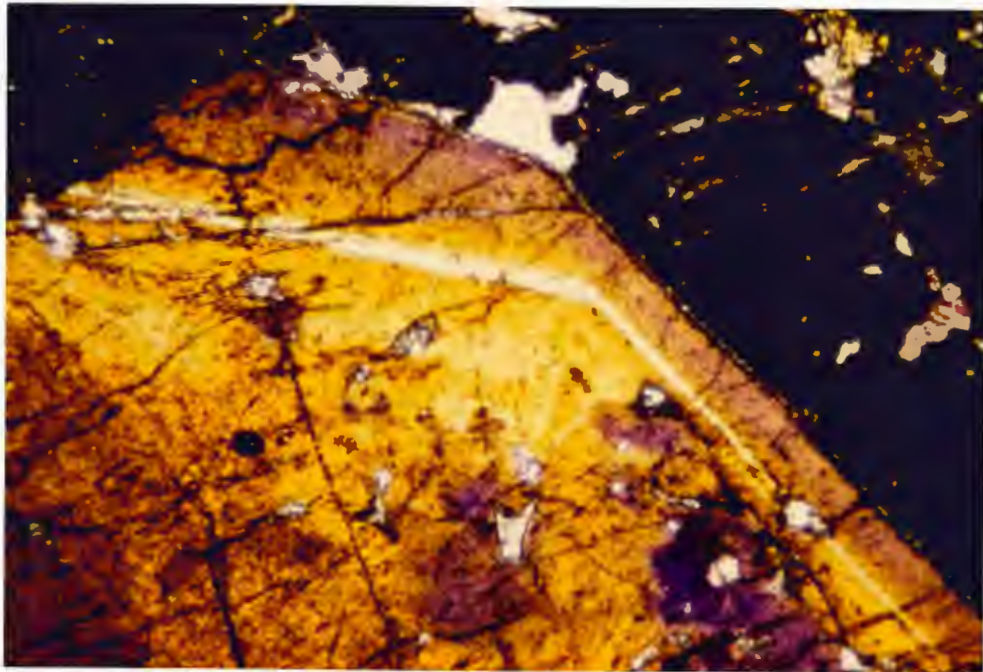


Figure 25. Photomicrograph of an idocrase grain showing color zonation. (Perdido Formation) Crossed polars. Field of view: 5.3 x 3.8 mm.

The Tin Mountain Formation was converted to a skarn along its southernmost exposure, where a 30 by 60 meter section is virtually surrounded by the quartz monzonite stock (Plate 1, Figure 22). At this location, dark greenish-brown skarn replaces silty limestone beds close to the intrusive contact. Idocrase and garnet are generally the predominant minerals within the skarn, forming large crystals (1 to 5 cm in diameter); in some areas they are the only minerals present. Diopside, tremolite and coarse-grained (4 to 6 mm in diameter) calcite are commonly present, with minor amounts of wollastonite (Figures 26 and 27, Table V).

#### Conditions of Metamorphism

The pressure attained during metamorphism is ascertained by using an overlying aggregate thickness of 1600 to 2000 meters for the overlying Paleozoic section in the district (McAllister, 1955). This yields a lithostatic pressure of about 1 kilobar.

Temperature of formation, and the mole fraction of  $\text{CO}_2$ , can be estimated by examining the variation in the mineral assemblages throughout the three metamorphic zones. A T-X diagram of pertinent stability fields and reactions, under isobaric conditions of 1 kilobar, is shown in Figure 28. From these isobaric equilibrium curves, the zone 1 assemblage of calcite-tremolite-quartz would form through reaction #1. The temperature at which this reaction would take place is dependent on the mole fraction of  $\text{CO}_2$  to  $\text{H}_2\text{O}$

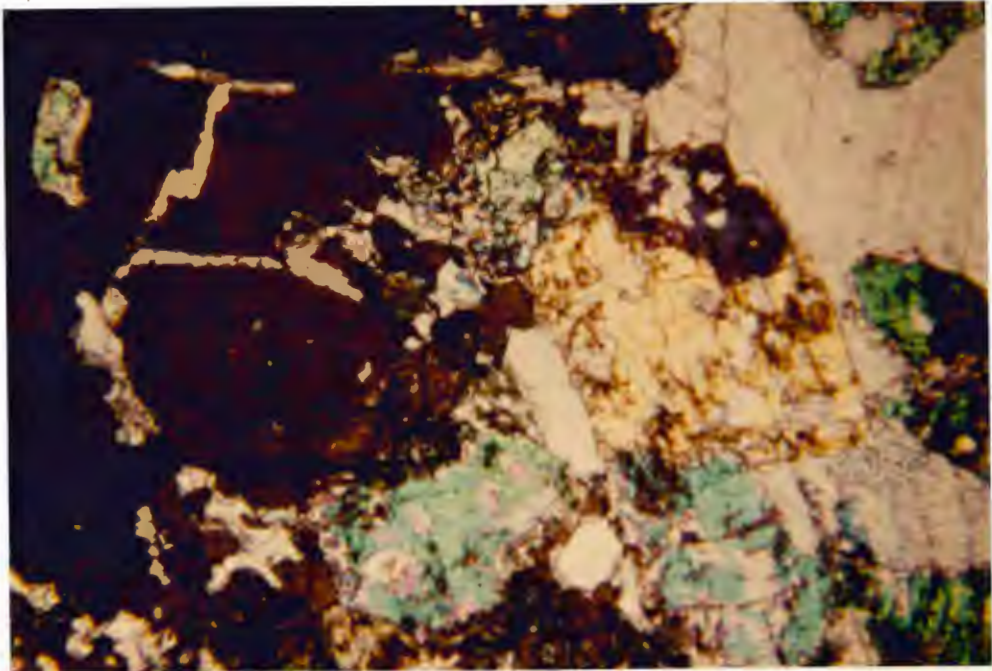


Figure 26. Photomicrograph of skarn mineralization in the Tin Mountain Formation. Note dark idocrase, highly birefringent diopside and gray calcite. Crossed polars. Field of view: 5.3 x 3.8 mm.

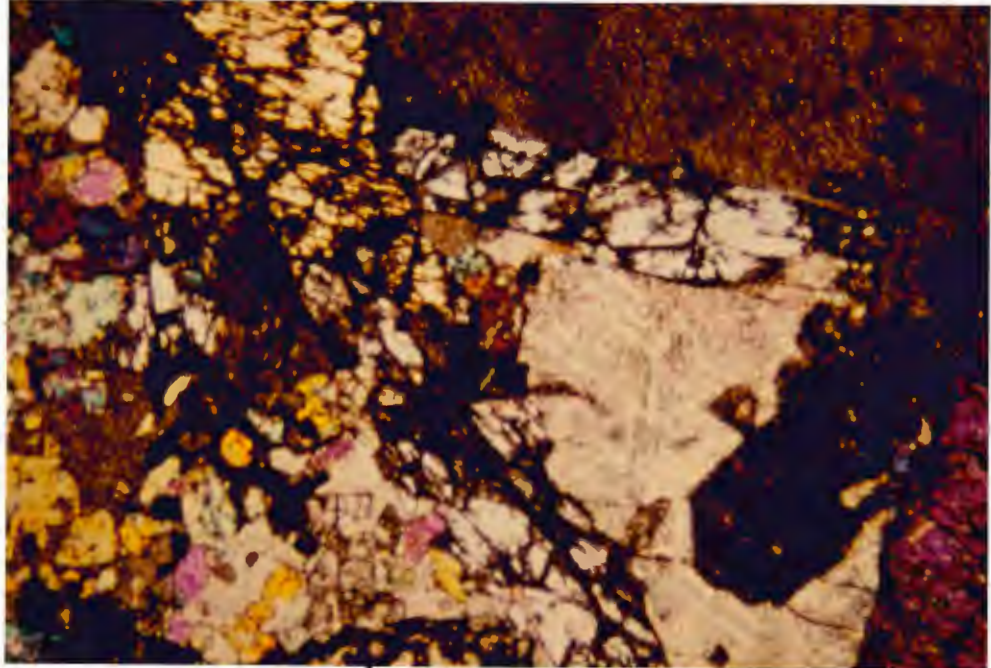


Figure 27. Photomicrograph of skarn mineralization in the Tin Mountain Formation. Note large wollastonite laths, highly birefringent diopside, calcite and black interstitial garnet. Crossed polars. Field of view: 5.3 x 3.8 mm.

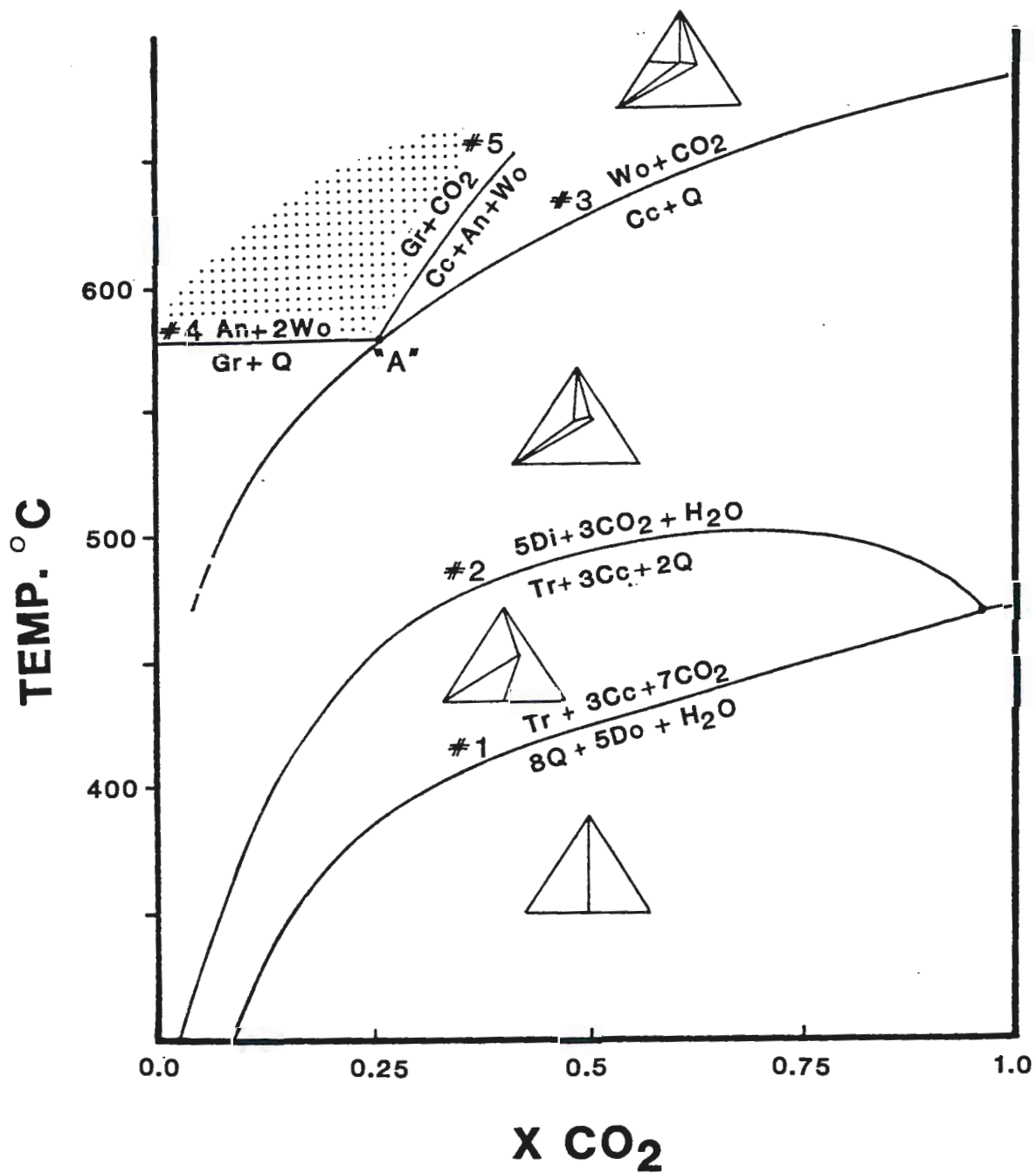


Figure 28. Schematic isobaric equilibrium curves for interpretation of calc-silicate assemblages. Symbols: Gr=grossular, Cc=calcite, Tr=tremolite, An=anorthite, Wo=wollastonite, Q=quartz, Do=dolomite (Greenwood, 1967; Kerrick, 1970; Skippen, 1974).



in the vapor phase. The temperature would range from approximately 320° C, at a X CO<sub>2</sub> of 0.1, to 460° C, at a X CO<sub>2</sub> of 0.9, with the assemblage being stable to temperatures of 420° C and 480° C at these two X CO<sub>2</sub> respectively. In zone 2 the common metamorphic assemblage of diopside-tremolite-quartz-calcite would develop through reaction #2. This reaction would take place within a temperature range of 390° C to 500° C at mole fractions CO<sub>2</sub> of 0.1 and 0.8 respectively, at 1 kilobar. The ACF diagram (Figure 29) shows the common mineral assemblages within zone 3; these are: a) wollastonite-diopside-grossular-calcite-quartz, b) wollastonite-diopside-grossular-anorthite-calcite, and c) idocrase-diopside-grossular-calcite. These assemblages are indicative of metamorphism under conditions of the pyroxene-hornfels facies.

From the T-X diagram (Figure 28) it can be seen that the formation of wollastonite, at a mole fraction of 0.25 CO<sub>2</sub>, occurs at the invariant point "A," at a temperature of approximately 580° C; sample 385 (Table V) would plot at this point. The assemblage of wollastonite-diopside-grossular-calcite (samples 269 and 296, Tables IV and V respectively) would plot in the stippled field of Figure 28, making 580° C the minimum temperature of formation, with the mole fraction of CO<sub>2</sub> in the vapor phase being less than 0.25. The major limiting reaction here is grossular + quartz → anorthite + 2 wollastonite, or equilibrium line #4. Sample 461 (Table V), with its assemblage of calcite-diopside-grossular-wollastonite-anorthite, would plot on the equilibrium line #5, also making the minimum

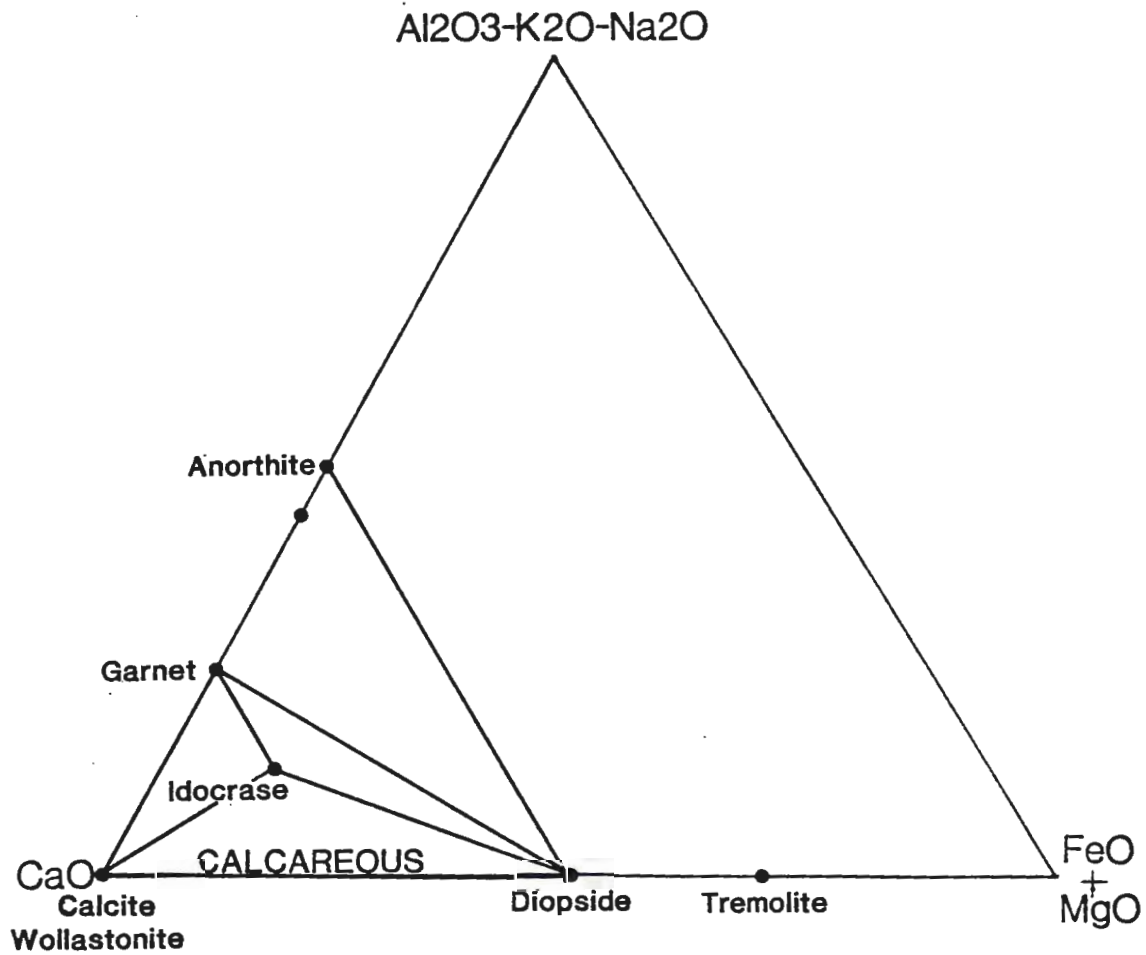


Figure 29. ACF diagram of the mineral assemblages present in Zone 3 calc-silicate rocks.

temperature of formation  $580^{\circ}$  C, with the mole fraction of  $\text{CO}_2$  being greater than 0.25 in this case.

### Dolomitization

Dolomitization is common in the Lost Burro and Tin Mountain Formations. The dolomitization is most common along or near faults, at crests of folds, and as a wall rock alteration adjacent to ore mineralization. The dolomite is a fine- to medium-grained (0.5 to 2 mm in diameter), buff- to tan-colored rock that forms patches and irregular shaped zones which often cross-cut the limestone bedding (Figure 30). The dolomite may have formed by hydrothermal alteration of the limestone either during or prior to ore formation. If dolomitization occurred prior to ore formation, the ore forming fluids may have used these dolomitized zones as permeable channels, due to the more porous nature of the dolomite (McAllister, 1955). Dolomitization will be discussed in more detail in the chapter on ore deposits.



Figure 30. Irregular shaped zone of dolomitization within the Lost Burro Formation. Average shrub is 40 cm in diameter.

## METASOMATISM WITHIN THE QUARTZ MONZONITE STOCK

The major quartz monzonite stock within the study area has not been extensively altered. However, adjacent to limestone contacts there has been an exchange of major elements between the intrusion and the metamorphosed limestones. Along these contacts, exposures range from a rock containing euhedral phenocrysts of perthitic orthoclase and microcline (0.5 to 1 cm in diameter), set in a groundmass of (0.5 to 1 mm in diameter) orthoclase, to a more normal quartz monzonite, partly replaced by diopside, wollastonite, garnet and calcite (Figure 31).

Five analyses of unaltered quartz monzonite, from the main stock to the south of the Defense Mine (Plate 1), were compared with one analysis of an altered quartz monzonite, from the contact between the stock and a small patch of Perdido Formation south of the Defense Mine (Plate 1). The results of the analyses are given in Table I. The most pronounced chemical changes which appear to have occurred between the altered and non-altered quartz monzonite are the depletion in  $\text{SiO}_2$  and  $\text{Al}_2\text{O}_3$ , and the apparent increase in CaO and MgO (Table I). Though no chemical analyses were made on the carbonate counterparts, these data suggest that the process of metasomatism has taken place, at least locally, along contacts between the quartz monzonite stock and the adjacent carbonate strata.

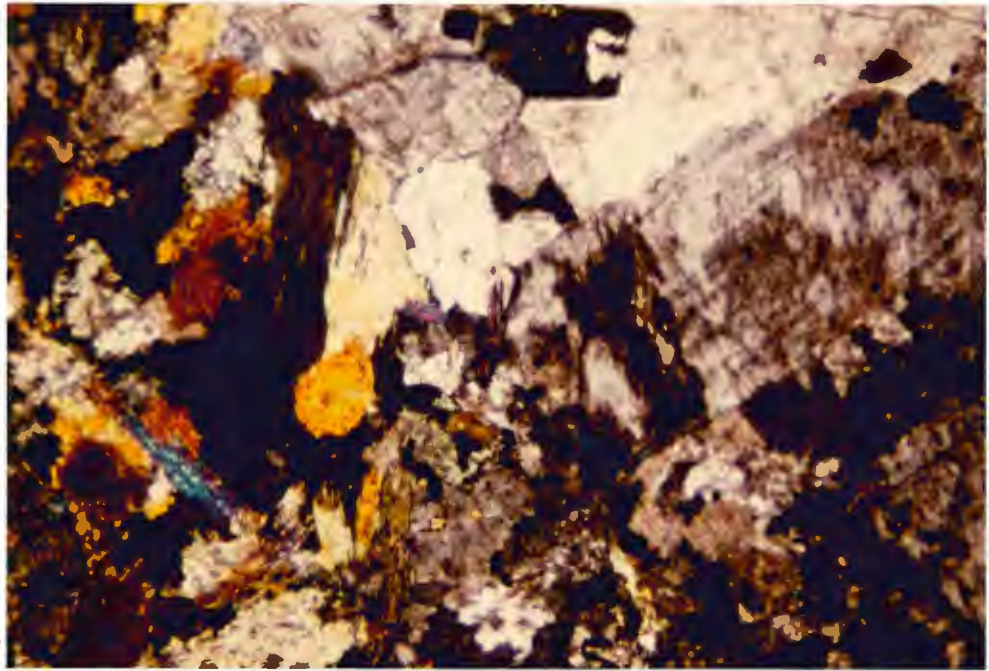


Figure 31. Photomicrograph of altered quartz monzonite near contact with Perdido Formation. Note diopside and garnet replacing feldspar. Crossed polars. Field of view: 5.3 x 3.8 mm.

TABLE I. Chemical Analyses of the Quartz Monzonite Stock

	<u>SiO2</u>	<u>Al2O3</u>	<u>MgO</u>	<u>K2O</u>	<u>Na2O</u>	<u>Fe2O3*</u>	<u>MnO</u>	<u>Ba</u>	<u>TiO2</u>	<u>P2O5</u>	<u>CaO</u>	<u>Total**</u>
<u>NON-ALTERED</u>												
273	65.74	16.74	1.98	3.55	2.78	1.54	.086	.072	.534	.270	6.70	100.00
359	62.50	16.74	1.94	4.12	2.83	5.76	.135	.080	.673	.442	4.75	100.00
390	62.50	17.34	1.74	4.45	2.82	4.88	.154	.086	.601	.456	4.97	100.00
605	61.79	17.29	2.09	4.57	2.71	5.50	.158	.088	.665	.429	4.71	100.00
607	61.20	17.30	1.89	4.50	2.60	5.75	.146	.080	.698	.414	5.44	100.00
<u>ALTERED</u>												
611	49.94	10.90	10.80	1.29	1.50	5.55	.150	.024	.361	1.820	17.64	100.00

\* Fe2O3 is total Fe

\*\* Weight % recalculated to 100%

## STRUCTURE

### INTRODUCTION

Structurally, the study area consists of folded Paleozoic carbonate rocks that are intruded by a quartz monzonite stock and interrupted by many faults (Figure 32, Plate 1). The first of three major structural events deformed the Paleozoic strata into broad anticlines trending N to N 30° W, and produced thrust faults at the Modoc and Minnietta Mine sites (Hall and Stephens, 1963). The second period of deformation was caused by forcible intrusion of the quartz monzonite stock. This event shouldered aside the carbonate rocks and overturned beds of the Perdido, Tin Mountain and Lost Burro Formations adjacent to the contacts. Intrusion was followed by a long period of erosion until the late Cenozoic, when extensive regional warping and accompanying strike-slip and normal-fault movement formed the east-tilted Argus Range (Hopper, 1947).

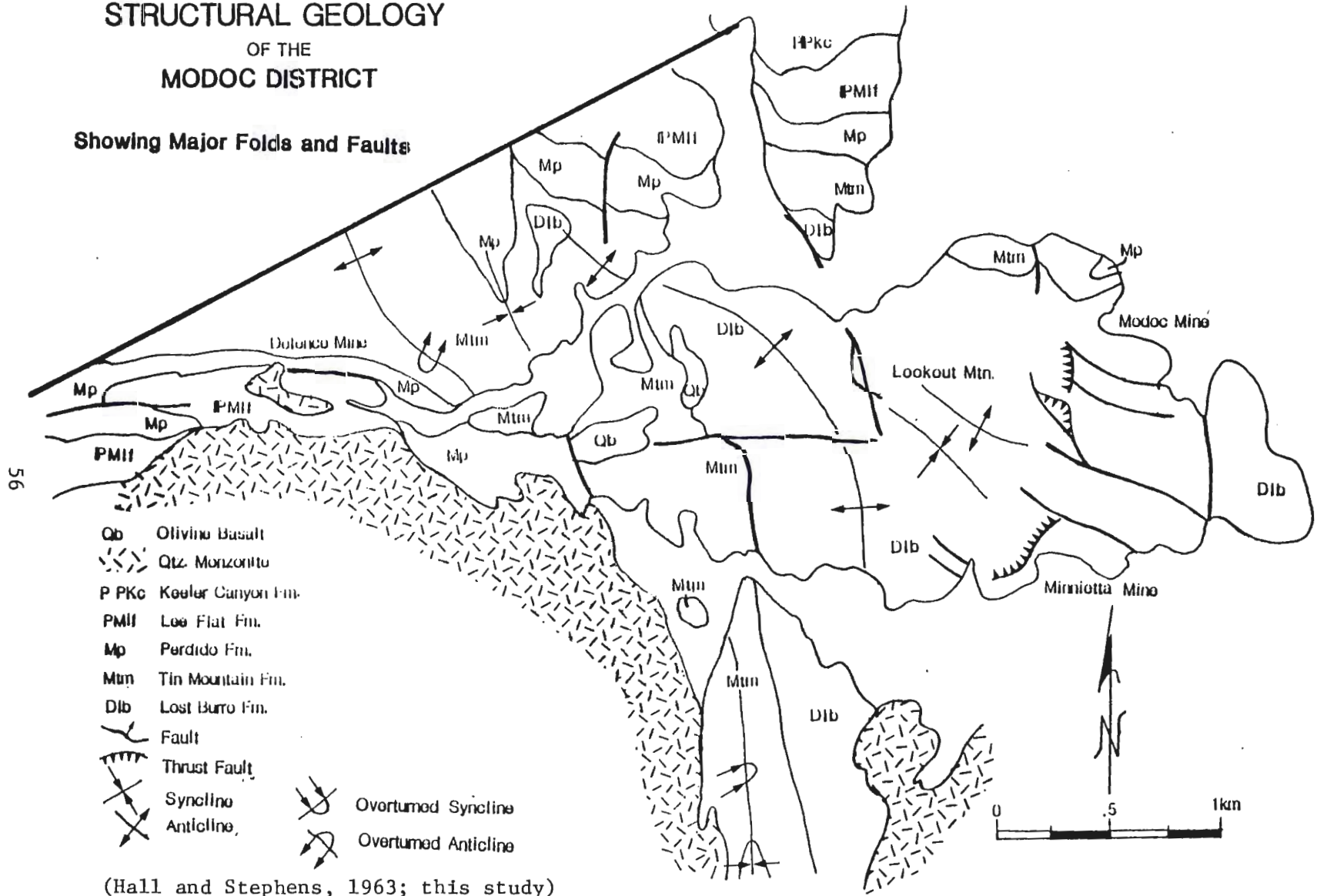
### FOLDS

One major anticline dominates the structure within the study area (Figure 33). The axis of this anticline trends NNW to SSW (Figure 32). North of the intrusion, the axis of this broad anticline is overturned adjacent to the contact, and tightly folded northeast of the Defense Mine (Figure 32, Plate 1). The Paleozoic rocks strike N 50° W to N 80° W and dip steeply northeast in the overturned section,



Figure 32.  
**STRUCTURAL GEOLOGY**  
 OF THE  
**MODOC DISTRICT**

Showing Major Folds and Faults



which is comprised of the Tin Mountain Formation to the north through the Perdido and Lee Flat Formations to the south. To the south, the anticline is displaced 1200 meters to the east by a fault and continues over Lookout Mountain. The Minnietta Mine is on the east limb of this large anticline. Bedding generally strikes northward and dips steeply to the east. The Modoc Mine area is also on the northeast limb of the major anticline, with bedding striking N 30° W to N 50° W and dipping 35° to 80° east. Locally, many small-scale folds are present on the limbs of the major anticline (Figure 32).

Adjacent to the east edge of the intrusion, in the southernmost portion of the study area, the Tin Mountain and Perdido Formations have been deformed into a syncline. This syncline has been subsequently overturned by the quartz monzonite stock (Figure 32). Overturned beds of the Tin Mountain and Lost Burro Formations strike northward and dip 45° to 80° east in this area. Small-scale isoclinal folds and drag folds are common locally along these limbs (Figure 34).

#### FAULTS

The most prominent faults within the study area trend northwest to west and extend from the Lost Burro Formation, east of the Minnietta Mine, across Lookout Mountain toward the Defense Mine (Figure 32). At the Defense Mine, the Tin Mountain and Perdido Formations are off-set by a series of northwest-striking faults which have

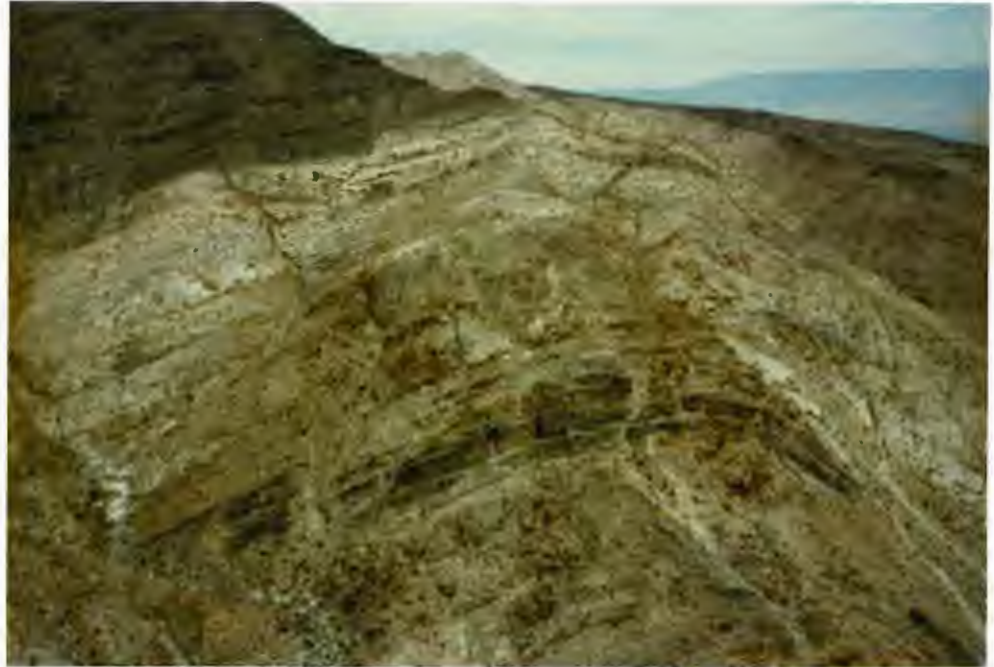


Figure 33. Looking north at the major anticline within the Tin Mountain Formation. Field of view approximately 1 km wide.



Figure 34. Drag folding within Lost Burro Formation. Note larger scale folding in background. Field of view of small scale fold is 2m.

conspicuous brecciated zones 0.5 to 1.5 meters thick, with a few as thick as 6 meters. A series of north-trending faults locally cut the Lost Burro Formation across Lookout Mountain (Figure 32).

Several small thrust faults were mapped at the Minnietta and Modoc Mine sites. In general these faults trend north-south and could be traced for 150 to 300 meters, with the upper plate being thrust eastward (Figure 32, Plate 1).

## LEAD, SILVER, ZINC ORE DEPOSITS

### DISTRIBUTION

Lead-silver-zinc deposits are concentrated in the Modoc District between Thompson Canyon and Stone Canyon (Plate 1). The principal mines are the Defense, located in the Tin Mountain Formation, and the Minnietta and Modoc located within the Lost Burro Formation (Plate 1). A number of prospects are also present to the north and west of the mapped area, but the mineralization associated with these is generally low grade and sporadic.

### SIZE AND CHARACTER OF ORE BODIES

The Pb-Ag-Zn ore bodies in the district are flat-lying, pod-shaped masses that have sharp contacts with the limestone host rock. They are small and high grade, with the principal primary ore mineral being argentiferous galena. Associated chalcopyrite, pyrite and sphalerite are present in small quantities (Table VII). Most of the ore bodies are partly to completely altered to supergene minerals, with cerussite and pyromorphite being the most common secondary lead minerals; manganese oxides are also abundant close to the surface. The ore in these near-surface deposits is a dark brown or black, fine-grained mixture of cerussite, cerargyrite, and relict galena, with jasper and pyrolusite.

The two largest ore bodies in the Defense Mine, the Upper and the Foreman deposits, contained about 12,000 tons of ore that averaged 20% lead and 17.5 ounces per ton silver (Hall and Stephens, 1963). Both ore bodies, which are now mostly mined out, were approximately 75 meters long, 3 to 20 meters wide, and 1 to 5 meters thick (Baker, 1963). The largest deposit in the Minnietta Mine is comparable in size to the above deposits. Within the Modoc Mine the Number Four ore body was probably the largest in the district. The Number Four ore body has been stoped for a strike length of 50 meters and has a maximum width of 20 meters for a vertical distance of about 55 meters (Hall and Stephens, 1963). Undoubtedly, several tens of thousands of tons of ore were mined from this deposit, but exact tonnages are not known. Most other ore bodies in the district are small with some pods in the Minnietta Mine containing only a few tons of ore; ore bodies of a few hundred tons in the Modoc District are common. The grade of ore mined from these small ore deposits was very high, averaging 46 to 62 ounces per ton silver and 17 to 20% lead (Crawford, 1894).

#### MINERALOGY

The minerals identified in this study, along with their chemical formulas, are listed in Table II. The modal mineralogy of the polished sections studied is also listed in Appendix B.

TABLE II. Minerals Identified (with chemical formulas)  
Within the Pb-Ag-Zn Deposits

HYPOGENE MINERALS

METALLIC MINERALS

Chalcopyrite	$\text{CuFeS}_2$
Galena	$\text{PbS}$
Native Silver	$\text{Ag}$
Pyrite	$\text{FeS}_2$
Sphalerite	$\text{ZnS}$
Tetrahedrite	$(\text{Cu,Fe})_{12}(\text{Sb-Ag})_4\text{S}_{13}$

GANGUE MINERALS

Calcite	$\text{CaCO}_3$
Chalcedony	$\text{SiO}_2$
Dolomite	$\text{MgCa}(\text{CO}_3)_2$
Jasper	$\text{SiO}_2$

SUPERGENE MINERALS

SULFIDE ZONE

Chalcocite	$\text{Cu}_2\text{S}$
Covellite	$\text{CuS}$
Digenite	$\text{Cu}_9\text{S}_5$
Stromeyerite	$(\text{Ag,Cu})_2\text{S}$

OXIDE ZONE

Bindheimite	$\text{Pb}_2\text{Sb}_2\text{O}_6(\text{O,OH})$
Cerargyrite	$\text{AgCl}$
Cerussite	$\text{PbCO}_3$
Coronadite	$\text{MnPbMn}_6\text{O}_{14}$
Hemimorphite	$\text{Zn}_4(\text{Si}_2\text{O}_7)(\text{OH})_2 \cdot \text{H}_2\text{O}$
Limonite	Hydrous Fe Oxide
Malachite	$\text{Cu}_2\text{CO}_3(\text{OH})_2$
Pyrolusite	$\text{MnO}_2$
Pyromorphite	$\text{Pb}_5(\text{PO}_4, \text{AsO}_4)_3\text{Cl}$

### Hypogene Minerals

The primary ore in the lead-silver deposits consists of medium- to coarse-grained (1 to 5 mm in diameter) galena with small amounts of pyrite, tetrahedrite, sphalerite, chalcopyrite and native silver, enclosed by a gangue composed of chalcedony, jasper, calcite and/or dolomite (Table XIII). Galena, with exsolution blebs of tetrahedrite, is by far the most abundant ore mineral (80 to 96%) (Figure 35). Pyrite, sphalerite, and chalcopyrite are sparsely disseminated throughout most of the polished sections studied. Sphalerite occurs as blebs (0.25 to 0.5 mm in diameter) in galena or as fine grains in the gangue material. The chalcopyrite occurs as minute blebs in sphalerite and has also apparently formed by exsolution (Figure 36); it commonly occurs where pyrite is present in the section (Figure 37).

### Gangue Minerals

Calcite and dolomite are the predominant gangue minerals in all of the lead-silver-zinc deposits of the district. Calcite is very abundant (70 to 80%), and ranges in color from milky white to brownish gray with rhombohedrons as much as four centimeters on a side. Dolomite within the Modoc and Minnietta Mines, the result of dolomitization of limestone, appears as a yellowish, fine- to medium-grained carbonate which weathers to a light brown color. Tan to light gray chaledony and dark, reddish brown jasper are also





Figure 35. Photomicrograph of gray tetrahedrite exsolution bleb in galena. Crossed polars. Field of view: 1.5 x 2.2 mm.

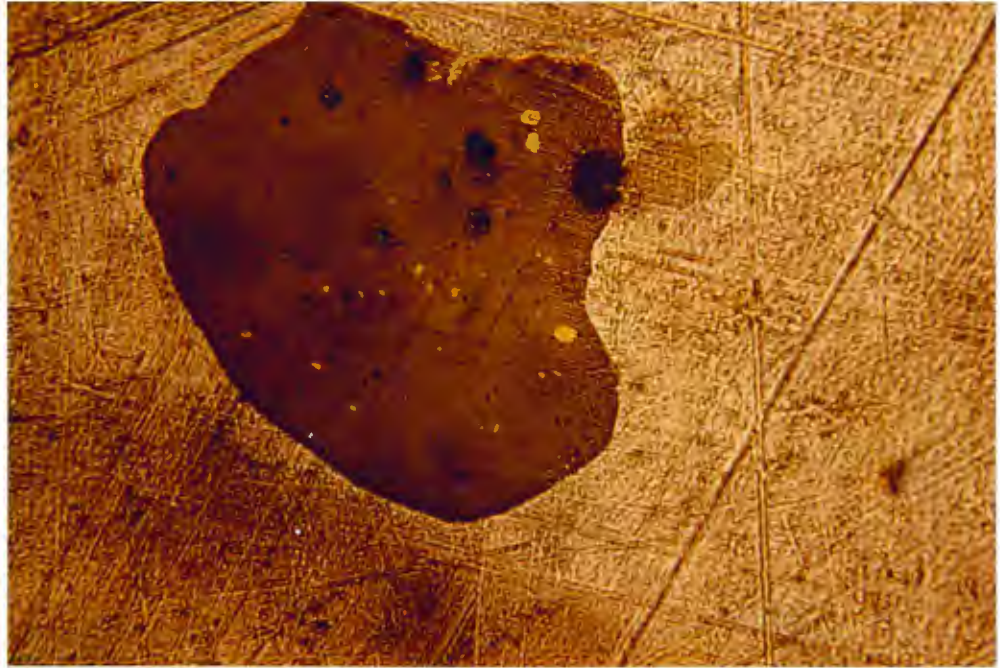


Figure 36. Photomicrograph of dark-gray sphalerite grain in galena. Note small yellow exsolution inclusions of chalcopyrite in sphalerite grain. Crossed polars. Field of view: 2.2 x 1.5 mm.

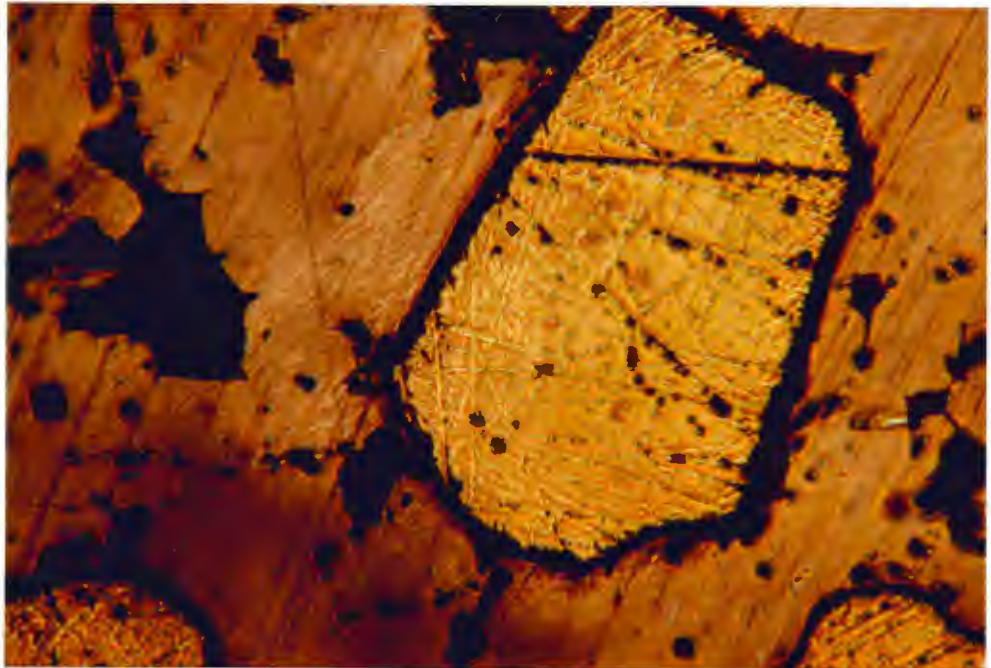


Figure 37. Photomicrograph of yellow pyrite grains in galena. Black is gangue. Crossed polars. Field of view: 2.2 x 1.5 mm.

common gangue minerals, which form cryptocrystalline masses in the stockwork veining that is associated with the ore mineralization.

### Supergene Minerals

Many of the ore bodies are partly altered to various supergene minerals. The sulfide minerals within the supergene ore consist predominantly of covellite, chalcocite and digenite. These minerals form feathery (tree-like) zones, along cleavage and fractures in relict galena, and fibrous intergrowths in the oxide minerals (Figures 38 and 39).

The oxide, supergene, ore minerals consist predominantly of cerussite, hemimorphite, bindheimite and cerargyrite which are set in a gangue of pyrolusite, coronadite, chalcedony and limonite. Minor relict galena remains in most oxide ore (Table XIII). Oxidized copper minerals are present locally in small amounts. Cerargyrite forms tiny olive-green cubes, and smears with a waxy luster along fracture surfaces. Cerussite is the principal secondary lead mineral formed from the oxidation of galena, but it is not common where the ore contains large amounts of manganese. Bindheimite is present in small amounts in most oxide ore containing cerussite and relict galena. It forms a yellow powdery coating on the cerussite.

An unequivocal primary source has not been found for the abundant manganese in the Modoc District supergene ores (Norman and Stewart,

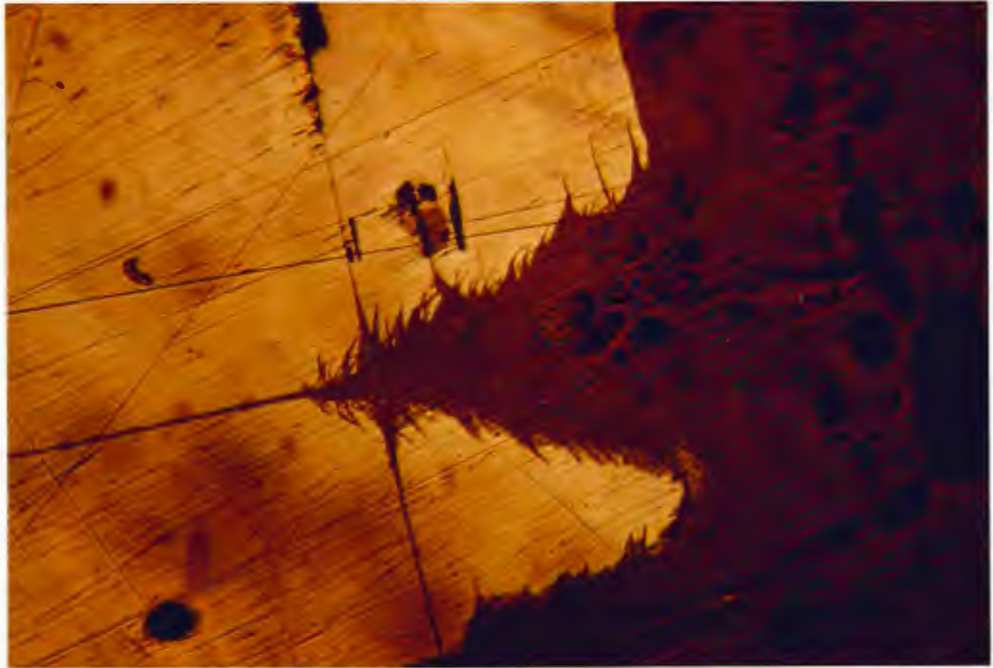


Figure 38. Photomicrograph of replacement texture between light gray galena and dark gangue. Secondary bluish covelite occurs along contact. Crossed polars. Field of view: 2.2 x 1.5 mm.



Figure 39. Photomicrograph of bluish covelite and dark gray chalcocite in galena (yellow). Crossed polars. Field of view: 2.2 x 1.5 mm.

1951). Black, sooty manganese oxide stains much of the rock and is abundant in fault zones at both the Modoc and Minnietta Mines. This manganese mineral was identified as coronadite by X-ray diffraction pattern and by X-ray spectrographic analysis (Fron del and Heinrich, 1942). It is a dense, massive, dark gray mineral with a conchoidal fracture. Pyrolusite is associated with the coronadite and also occurs as fine-grained black, sooty coatings along faults, near the ore deposits. Numerous attempts were made by the author to identify, by X-ray diffraction, the black, sooty minerals in hand samples collected near these fault zones. These attempts met with little success due to the amorphous nature of the minerals. They are assumed to be amorphous Fe-Mn oxides.

#### Primary Source of the Silver

As noted earlier, many zones within the ore deposits of the district have relatively high silver grades (up to 100 ounces per ton). Secondary supergene enrichment accounts for much of this very high silver content, though an initial, primary source of the silver must be considered. Very little native silver was observed in the ore samples. This suggests that the silver is within the galena itself, as a solid solution with  $Pb_2S$  and  $Ag_2S$ , or within the tetrahedrite, as a solid solution between the tetrahedrite-freibergite series. The silver content, which is almost always present in galena, consists of up to a maximum of 0.1% solid solution  $Ag_2S$  (Hall, 1959). The term freibergite has been loosely

applied to tetrahedrite with varying silver content. A study done on the Mount Isa Pb-Zn-Ag ore bodies of Queensland, Australia (Riley, 1974), concluded that a maximum silver content of approximately 51 wt. % Ag can be reached via a replacement of copper by silver in freibergite. It is thought here that the primary silver content at the Modoc District ore bodies is from both the silver within the galena as  $Ag_2S$ , and the tetrahedrite-freibergite series minerals.

#### ORE CONTROLS

The lead-silver deposits are localized in the carbonate rocks, close to contacts with the quartz monzonite plutons. There have been no producing lead-silver mines more than 2.5 km from a quartz monzonite pluton (Hall and Stephens, 1963).

In addition to being localized near intrusive contacts, the deposits have a distinct stratigraphic control. Pure limestone recrystallized to marble is the most favorable host rock in the Modoc District. The Lost Burro Formation of Devonian age, and Tin Mountain limestone of Mississippian age, both relatively pure limestones that have been recrystallized to marble, contain ore deposits. The Modoc and Minnietta Mines are situated in the Lost Burro Formation; whereas, the Defense Mine is in the Tin Mountain limestone. It is apparent from this localization of mineralization, that relatively pure marble of Devonian and Mississippian age is more favorable for ore deposition, than silty limestones of Pennsylvanian and Permian age

formations.

Within the relatively pure limestones and marbles, structural control is paramount in the actual location of all the lead-silver deposits. Fold hinges, faults and flat structures are favorable sites for deposition of the ore mineralization. Most of the known ore bodies are localized in flat sheeted zones termed flat structures, by Baker (1963). Goodwin (1957) suggests that these flat structures may be tension release fractures opened up between steep faults. They are the main ore control within the Defense Mine. At the Minnietta and Modoc Mines, however, thrust faults are the important ore controls. The thrusts appear to be an integral part of the system which enabled mineralizing fluids to be transported to favorable steeply dipping fault systems, and other structurally prepared areas. Anticlinal structures play an important role at the Surprise Mine north of the mapped area (Baker, 1963). The intersection of crests of anticlinal folds with steep faults are the important factors for ore localization within the district.

#### WALL ROCK ALTERATION

In general, there is no distinct zone of alteration adjacent to the lead-silver ore bodies. However, at both the Modoc and Minnietta Mines, white marble or light gray limestone host rock has taken on a distinct yellowish color on fresh surfaces; it weathers to a light brown. This color change is, in part, due to dolomitization of the

limestone and, in part, due to disseminated limonite in the marble. In the field the altered rock had to be tested with dilute hydrochloric acid to differentiate the limonite-rich, brown-stained marble from the brownish dolomitized marble. In thin section, however, the distinction is easily recognized (Figures 40 and 41). The dolomitization is extensive along faults close to the ore bodies, and pervades the marble near thrust faults at the Modoc Mine. This extensive dolomitization is most likely due to hydrothermal solutions entering the limestone at a relatively high temperature (Holland and Sergey, 1979). Such a solution may have Ca/Mg ratios within the stability range of dolomite, rather than that of calcite. On entering the limestone, this solution will react with calcite until the Ca/Mg ratio has risen to the value at the dolomite-calcite boundary (Figure 42), thus forming dolomite (Rosenberg and Holland, 1964).

Black manganese oxides occur within the dolomitized marble along the major thrust faults at the Minnietta and Modoc Mines, and along surface faults at the Defense Mine. The distribution of the black manganese oxides along faults and near ore bodies suggests that the original manganese may have been introduced at the time of dolomitization.



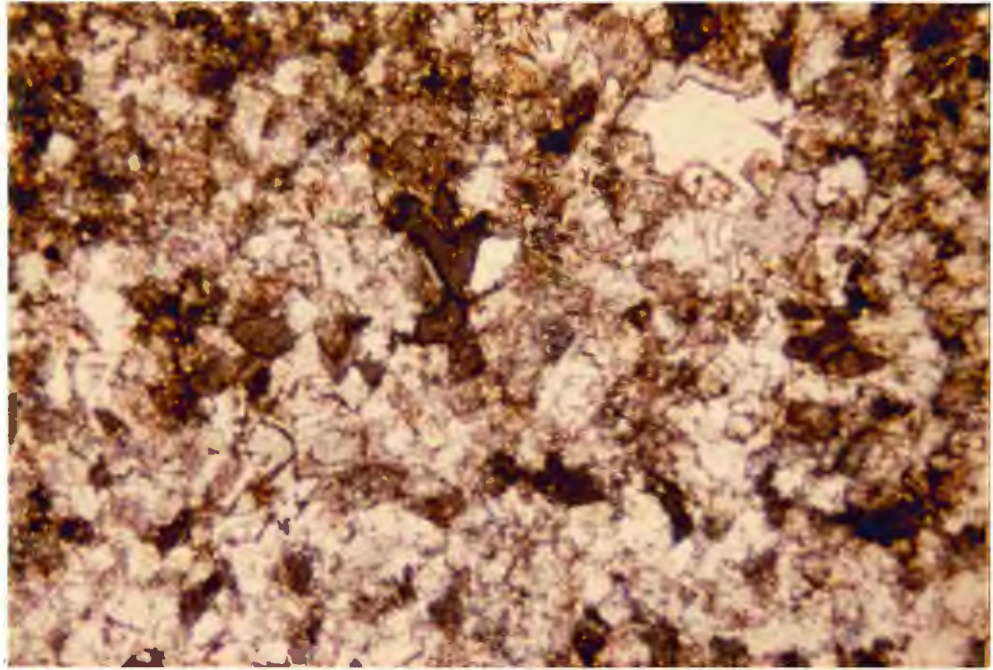


Figure 40. Photomicrograph of dolomite found in alteration zones adjacent to Ag ore within the Lost Burro Formation. Crossed polars. Field of view: 5.3 x 3.8 mm.

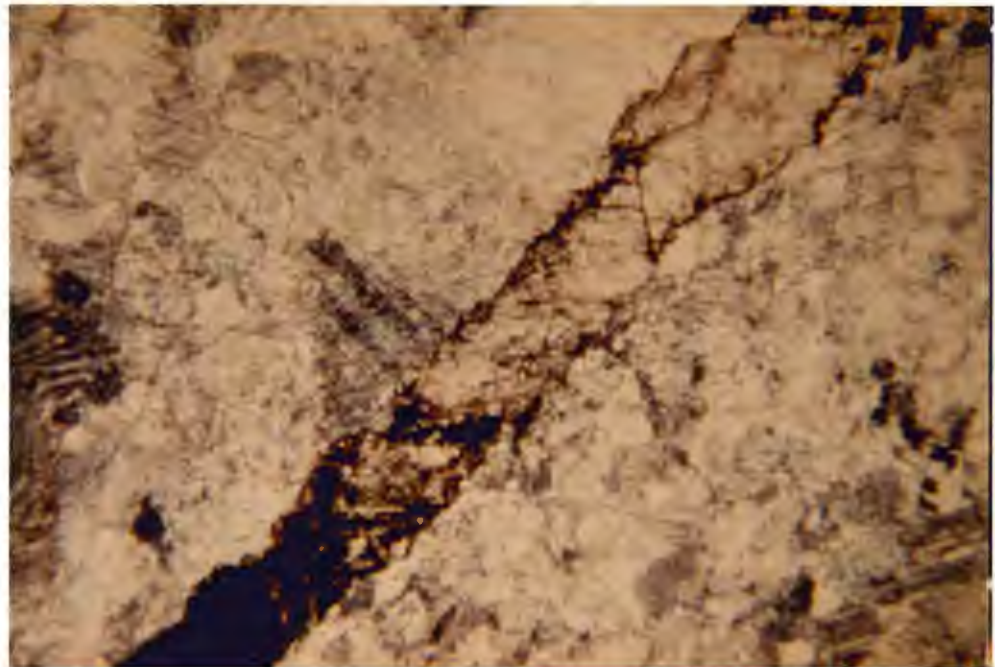


Figure 41. Photomicrograph of dolomite vein in calcite. Plane polarized light. Field of view: 5.3 x 3.8 mm.

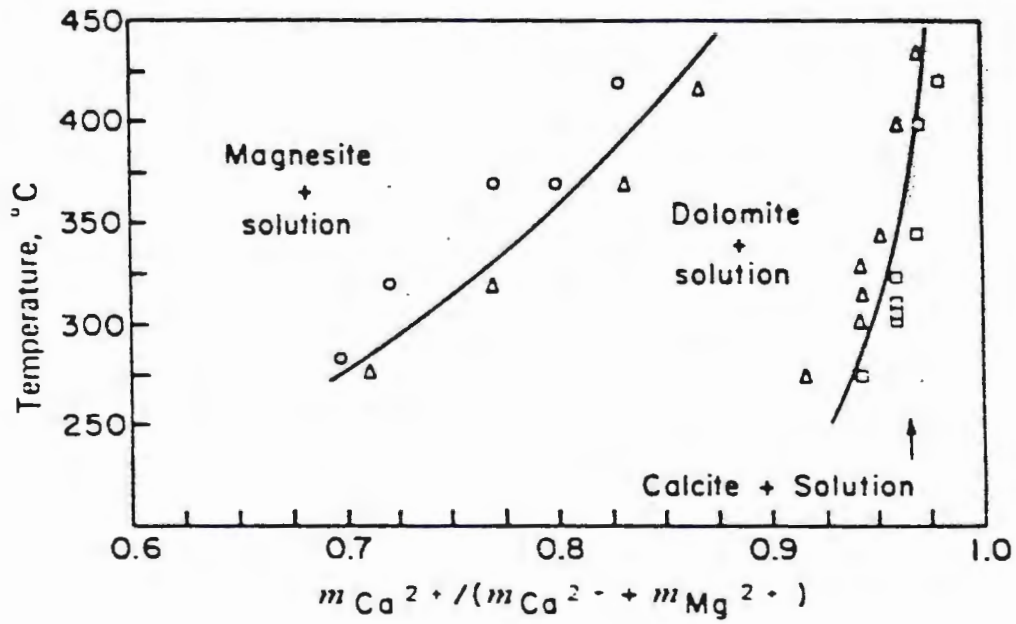


Figure 42. The mole fraction  $m_{Ca^{2+}} / (m_{Ca^{2+}} + m_{Mg^{2+}})$  in solutions in equilibrium with calcite + dolomite and magnesite + dolomite at temperatures between 275 and 420 C. Triangles indicate runs in which calcite or magnesite was replaced by dolomite (Rosenberg and Holland, 1964).

## MODEL OF ORE GENESIS

There are broad similarities to all of the Pb-Ag-Zn ore deposits which have been found throughout southeastern California. Some of the more important of these are: A) association with granitic plutons, B) massive replacement-type argentiferous galena and sphalerite as ore, and C) structural control of ore deposits. However, detailed studies of these deposits have shown that each is unique in its ore genesis.

The Darwin Mine, for example, 10 km west of the Modoc District (Figure 1), is a Pb-Ag-Zn ore deposit which has been compared to the Modoc District deposits (Fiannaca, 1981). At Darwin, a quartz monzonite stock has been intruded into limestone of Pennsylvanian age. Adjacent to the stock, a metamorphic aureole (50 - 600 m) of calc-silicate rocks has developed, though the original bedding has been retained. Field relations, coupled with petrographic and chemical evidence by Kelley (1937), indicated that metasomatism played a dominant role in the formation of the calc-silicate aureole. The deposition of the ore bodies took place after a later period of tectonic fracturing, at which time large amounts of silica and metals were introduced into the contact skarn zone by hydrothermal solutions. These solutions are considered to have been magmatic in origin (White, 1974).

Though the similarities between the Darwin and Modoc ore deposits are

clear, there are also many differences. The ore within the Modoc District is located in non-metamorphosed, pure limestones of the Lost Burro and Tin Mountain Formations; whereas, the ore in the Darwin District is within the Lee Flat and Keeler Canyon Formations which were metamorphosed to skarn mineralization prior to ore deposition.

The quartz monzonite stock within the Modoc District was partially consolidated at the time of its emplacement, leading to brittle deformation of the surrounding carbonate rock; whereas, the quartz monzonite intrusion in the Darwin District was much more fluid, resulting in very little tectonic disturbance of the limestone country rock. Here, the stock was emplaced along bedding planes and pre-existing fractures. These differences suggest a difference in the nature of the hydrothermal solutions and a different source for the metals at each deposit.

It is beyond the scope of this study to outline the many possible combinations of sources of waters, metals, and precipitating mechanisms which could have taken place in the Modoc District. Rather, through field observations coupled with petrographic evidence from this study, and the comparison of the Modoc with the Darwin District, the following is an attempt to produce one possible model for the ore genesis of the Modoc Pb-Ag-Zn deposits.

The model proposed for the generation of the Pb-Ag-Zn ore bodies is one of meteoric-connate (+ 5% magmatic component) hydrothermal

solutions set into convective circulation by the interaction with the igneous intrusion. High salinity solutions in this convection cell leached metals from the surrounding country rock and carried the metals as metal-chloride complexes. As these hydrothermal solutions migrated upward/outward they decreased in temperature and salinity, and possibly increased in pH (Barnes, 1979), thus precipitating out the metals in structurally prepared areas within the pure limestones of the district.

## CONCLUSIONS

1) The Modoc District consists of a sequence of complexly folded and faulted Paleozoic, marine carbonate rocks, which have undergone further deformation and metamorphism by the forcible intrusion of a quartz monzonite stock. The forcible nature of this intrusion is supported by the shattering and deformation of the carbonate strata adjacent to the intrusive contacts, and the sharp contacts between the stock and carbonate rocks.

2) Heat generated from the quartz monzonite intrusion formed a contact metamorphic aureole around the stock. Both metamorphic and metasomatic processes have taken place within the surrounding carbonate country rocks. The contact metamorphism can be divided into three distinct zones of differing metamorphic facies: zone 1 (albite-epidote facies) developed from 2.5 km to 700 meters away from the stock; zone 2 (hornblende-hornfels facies) developed from 700 to 30 meters away; and zone 3 (pyroxene-hornfels facies) developed from the contact, outward, for 30 meters.

3) Hydrothermally generated Pb-Ag-Zn ore deposits occur within the relatively non-metamorphosed limestones of the Lost Burro and Tin Mountain Formations. They occur as small, high-grade bodies in structurally controlled, flat-lying pods and irregular, tabular masses. Hydrothermal solutions, channeled through faults and

fractures, precipitated the metals at appropriate temperatures, pressure and pH conditions, in structurally prepared areas. There is no association between the ore mineralization and the metamorphic skarn mineralization within the district.

4) The primary ore consists largely of argentiferous galena and tetrahedrite, with minor pyrite, sphalerite, and chalcopyrite within a gangue of jasperoid, dolomite, and calcite. Typically abundant supergene minerals include cerargyrite, cerussite, covellite, chalcocite and various Pb-Fe-Mn oxides. Alteration is closely associated with ore mineralization and is not widespread; it includes dolomitization, occasional addition of silica, and alteration to manganese minerals.

5) The silver within the ore rock of the Modoc District is within both: a) the galena itself, as a solid solution between  $Pb_2S$  and  $Ag_2S$ , and b) the associated tetrahedrite, as a solid solution between the tetrahedrite-freibergite series minerals.

6) The manganese alteration and dolomitization of the wall rock, adjacent to the ore bodies within the district, was caused by hydrothermal solutions at the time of ore deposition.

7) A model of ore genesis has been proposed, in which hydrothermal solutions of meteoric-connate origin are set into convective circulation by the heat supplied by the quartz monzonite stock. These

hydrothermal solutions leached metals from the surrounding country rock, carrying them as metal-chloride complexes. As the solutions migrated upward, they decreased in temperature and in salinity; this triggered precipitation of the metals within structurally prepared areas in the Lost Burro and Tin Mountain Formations.



#### REFERENCES CITED

- Bailey, E.H. and Stevens, R.E., 1960. Selective staining of K-feldspar and plagioclase on rock slabs and thin sections: Am. Mineralogist, v.45, p.1020-1025.
- Baker, A., 1963. Defense Mine, Modoc District, Inyo County, California (unpublished report): Panamint Mining Co., 23 p.
- Barnes, H.L., 1979. Solubilities of ore minerals, in Barnes, H.L., ed., Geochemistry of Hydrothermal Ore Deposits (second edition): New York, John Wiley, p.404-460.
- Chapman, P., 1980. Memorandum to M. Easdon, Modoc Silver Property, Inyo County, California (unpublished report): Lacana Mining Inc., 5 p.
- Chayes, Felix, 1952. Notes on the staining of potassium feldspar with sodium cobaltinitrite in thin section: Am. Mineralogist, v.37, p.337-340.
- Crawford, J.J., 1894. Argentiferous galena - Inyo County, California: California Min. Bur. Rept. 12 (Second Biennial), p.23-25.
- Fiannaca, M., 1981. Reconnaissance exploration of Argus Mountains, Inyo County, California (unpublished report): Lacana Mining, Inc., 8 p.
- Friedman, G.M., 1959. Identification of carbonate minerals by staining methods: J. Sed. Petrology, v.29, p.87-97.
- Frondel, Clifford and Heinrich, E.W., 1942. New data on hetaerolite, hydrohetaerolite, coronadite and hollandite: Am. Mineralogist, v.27, p.48, 56.
- Goodwin, J.G., 1957. Lead and zinc in California: California J. Mines and Geology, v.53, p.504.
- Greenwood, H.J., 1967. Wollastonite: stability in H<sub>2</sub>O-CO<sub>2</sub> mixtures and occurrence in a contact-metamorphic aureole near Salmo, British Columbia, Canada: Am. Mineralogist, v.52, p.1669-1680.
- Hall, W.E., 1959. Geochemistry study of Pb-Ag-Zn ore from the Darwin Mine, Inyo County, California: Mining Eng., v.11, no.9, p.940.
- Hall, W.E. and MacKevett, E.M., 1958. Economic geology of the Darwin Quadrangle, Inyo County, California: California Div. Mines and Geology Spec. Rept. 51, 87 p.

- Hall, W.E. and Stephens, H.G., 1963. Economic geology of the Panamint Butte Quadrangle and Modoc District, Inyo County, California: California Div. Mines and Geology Spec. Rept. 73., 39 p.
- Heinrich, E. Wm., 1965. Microscopic Identification of Minerals: New York, McGraw-Hill, p.358-356.
- Holland, H.D. and Sergej, M.D., 1979. The solubility and occurrence of non-ore minerals, in H.L. Barnes, ed., Geochemistry of Hydrothermal Ore Deposits: New York, John Wiley, p. 461-508.
- Hopper, R.H., 1947. Geologic section from the Sierra Nevada to Death Valley, California: Geol. Soc. Am. Bull., v.58, no.5, p. 393-432.
- Jennings, C.W. 1958. Geologic map of California, Olaf P. Jenkins edition, Death Valley Sheet: California Div. Mines.
- Kelley, V.C., 1937. Origin of the Darwin silver lead deposits: Econ. Geol., v.32, no.8, p.987-1008.
- Kerrick, D.M., 1970. Contact metamorphism in some areas of the Sierra Nevada, California: Geol. Soc. Am., v.81, p.2913-2937.
- King, C.R., 1957. Memorandum upon the Minnietta Mine (unpublished report): Lacana Mining, Inc., 4 p.
- McAllister, J.F., 1952. Rocks and structure of the Quartz Spring area, Northern Panamint Range, California: California Div. Mines and Geology Spec. Rept. 25, 38 p.
- , 1955. Geology of mineral deposits in the Ubehebe Park Quadrangle, Inyo County, California: California Div. Mines and Geology Spec. Rept. 42, 63 p.
- Merriam, C.W., and Hall, W.E., 1957. Pennsylvanian and Permian rocks of the Southern Inyo Mountains, California: U.S. Geol. Surv. Bull. 1061-A., p.62
- Moore, J.G., and Hopson, C.A., 1961. The Independence Dike Swarm in Eastern California: Am. J. Sci., v.259, p.241-259.
- Norman, L.A., Jr., and Stewart, R.M., 1951. Mines and mineral resources of Inyo County: California J. Mines and Geology, v.47, p.17-233.
- Riley, J.F., 1974. The Tetrahedrite-Freibergite Series, with reference to the Mount Isa Pb-Zn-Ag Orebody: Mineral. Deposita (Berl.), v.9, p.117-124.

- Rosenberg, P.E. and Holland, H.D., 1964. Calcite-dolomite-magnesite stability relations in solutions at elevated temperatures: Science, v.145, p.700-701.
- Rosenblum, Samuel, 1956. Improved technique for staining potash feldspars: Am. Mineralogist, v.41, p.662-664.
- Skippen, G. 1974. An experimental model for low pressure metamorphism of siliceous dolomitic marble: Am. J. Sci., v.274, p.487-509.
- Tucker, W.B., and Sampson, R.J. 1938. Mineral resources of Inyo County, in thirty-fourth report of The State Mineralogist: California J. Mines and Geology, v.34, p.368-500.
- Turner, F.J., 1958. Mineral assemblages of individual metamorphic facies, in metamorphic reactions and metamorphic facies: Geol. Soc. Am., Memoir 73, p.199-237.
- Waring, C.A., and Huguenin, Emile, 1919. Inyo County in fifteenth report of The State Mineralogist: California Min. Bur. Annual Rept. 15, p.29-134.
- White, D.E., 1974. Diverse origins of hydrothermal ore fluids: Econ. Geol., v.69, p.954-973.

APPENDIX A. Modal Compositions of Rock Units

The following tables give modal compositions and textures of lithologic units as observed in thin section.

<u>Mineral</u>	<u>Abbreviation</u>	<u>Texture</u>	<u>Abbreviation</u>
Apatite	APA	Breccia	Bx
Augite	AUG	Felty Groundmass	Ft
Biotite	BIO	Foliated	Fo
Brucite	BRU	Fossil	F
Calcite	CAL	Granophyric	Gr
Chlorite	CHL	Holocrystalline	Ho
Clinopyroxene	CPX	Hornfels	H
Diopside	DIO	Hypidiomorphic	Hy
Dolomite	DOL	Micrite	M
Epidote	EPI	Myrmekitic	My
Garnet	GAR	Poikilitic	P
Hematite	HEM	Recrystallized	Rx
Hornblende	HB	Replacement	R
Idocrase	IDO	Skeletal Grains	Sk
Limonite	LIM	Sparite	S
Magnetite	MAG	Styolites	St
Malachite	MAL	Vein	V
Manganese Oxide	MOX		
Microcline	MIC		
Muscovite	MUS		
Olivine	OLI		
Orthoclase	ORT		
Plagioclase	PLG		
Potassium Feldspar	KSP		
Pyrite	PYR		
Quartz	QTZ		
Scapolite	SCP		
Sericite	SER		
Sphene	SPH		
Tremolite	TRE		
Wollastonite	WOL		
Zircon	ZIR		

Modal values are estimated and are listed in percent (%).

TABLE III. Modal Compositions of the Lost Burro Formation

T.S.#	ROCK NAME	TEXTURE	CAL	QTZ	DOL	TRE	DIO	MUS	HEM	MAG	LIM	OTHER
1A	Marble	S,Rx	99			1		Tr				
23	Limestone	S	99	.5				Tr	Tr			
24	Limestone	F,V,S	90	10		Tr						
25	Marble	S,Rx	99.9									Tr MOX
31	Marble	S	99	.5		Tr			.5			
37	Limestone	M,V	99	Tr						Tr		Tr BRU
40	Marble	S,Rx	94	Tr						2	4	
42	LS Breccia	Bx	98	1		1				Tr		
110A	Limestone	Rx,Fo	75	3		20			1		Tr	
143	LS Breccia	Bx	87			8			1		4	
182A	Limestone	S,Fo	99	.9								Tr ZIR
208A	Quartzite	Rx,V	4	92		3	Tr					Tr ZIR
208B	Quartzite	V	4	70		15	2		Tr			
210	Limestone	Rx,S	99	.6		.4						
233A	Limestone	S,Fo	96				1.5		Tr			2 SCP
233B	Marble	S,Rx	99					1		Tr		
233C	Dolomite	S,Rx			99	.5				Tr		
278	Marble	S,Rx	98	.5						.5	1	
414	Marble	St	99	Tr				Tr		Tr		Tr MOX
439	Limestone	S	99					1				
482	Dolomite	S			99.9				Tr			
500	Limestone	S	99	.5				Tr			Tr	
527	Limestone	M	95	.5		5			.5			
560	Limestone	S	98	2								
582	Limestone	S	98						1	1		
585	Marble	S,Rx	99.9					Tr				
593	Dolomite	S	35		60				1		4	
596B	Limestone	S,Rx	69	28					2			1 MAL

A-2

TABLE IV. Modal Compositions of the Tin Mountain Formation

<u>T.S.#</u>	<u>ROCK NAME</u>	<u>TEXTURE</u>	<u>CAL</u>	<u>TRE</u>	<u>DIO</u>	<u>MUS</u>	<u>IDO</u>	<u>GAR</u>	<u>QTZ</u>	<u>MAG</u>	<u>HEM</u>	<u>WOL</u>	<u>LIM</u>	<u>OTHER</u>
240	Skarn	P	14		45	1	40							Tr BRU
258A	Marble	Fo,Rx,S	100							Tr				
258B	Limestone	Bx	68						2				30	
259	Limestone	Rx	96		2				1	Tr	Tr			
261	Marble	Rx,S	100							Tr				
265	Skarn	P	15		40		45							
268B	Limestone	Bx	98						1	.5	.5			
269	Skarn	P	9		50			16				25		
303	Marble	S	100								Tr			
334	Limestone	Bx	97								1		2	
375	Limestone	F,S,V	99			1				Tr				
436	Limestone	V	80										20	
449	Limestone	F,M	98	Tr		1			1	Tr				
453	Limestone	S	70	.5					30					Tr PYR
486	Marble	S,Rx	99			Tr					Tr			
510	Limestone	S	92	2	4				1					
515	Limestone	S,Sk	99	.5									.5	
SK1	Skarn	P	22		28		46	8						

TABLE V. Modal Compositions of the Perdido Formation

<u>T.S.#</u>	<u>ROCK NAME</u>	<u>TEXTURE</u>	<u>CAL</u>	<u>QTZ</u>	<u>TRE</u>	<u>DIO</u>	<u>IDO</u>	<u>GAR</u>	<u>WOL</u>	<u>PLG</u>	<u>APA</u>	<u>ORT</u>	<u>OTHER</u>
296	Skarn	P,R	20			42		8	30				Tr MAG
309B	Limestone	S	94	1	.5	3.5					Tr		Tr ZIR
314	Skarn	R	4			46			8			42	
317	Hornfels	R,H	6	2		45		15		4		25	2 SPH
363	Skarn	H	36		8	22	28	6					
385	Hornfels	H	10	2		36		8	40	4	Tr		
387	Hornfels	F,H		44		50				5	1		
458	Skarn	P,R	18	Tr		52		8	20				Tr MAG
461	Skarn	R	12			32		4	36	16			
492	Limestone	M,V	70	30									
493	Limestone	M,V	15	85									
518	Limestone	S,V	94	3	1	2							Tr MAG
613	Skarn	R,P	15			47	33	5					

TABLE VI. Modal Compositions of Lee Flat Limestone

<u>T.S.#.</u>	<u>ROCK NAME</u>	<u>TEXTURE</u>	<u>CAL</u>	<u>QTZ</u>	<u>LIM</u>	<u>HEM</u>	<u>MAG</u>	<u>OTHER</u>
288B	Marble	Rx,S	99.9			Tr		
313B	Marble	Rx,S	100				Tr	
318B	Limestone	F,Bx	100			Tr		Organic
331	Marble	Rx,S	99	Tr			Tr	
466	Limestone	S,V	98	Tr			1	
491	Marble	Rx,S	98		2		Tr	
578	Marble	Bx	88	12				

A-5

TABLE VII. Modal Compositions of the Keeler Canyon Formation

<u>T.S.#</u>	<u>ROCK NAME</u>	<u>TEXTURE</u>	<u>CAL</u>	<u>QTZ</u>	<u>HEM</u>
497	Limestone	F,M (V,S)	84	14	2
498	Limestone	M (V,S)	73	23	4
499	Limestone	F	78	18	5



TABLE VIII. Modal Compositions of Hornblende-Biotite-Quartz Monzonite

<u>T.S.#</u>	<u>TEXTURE</u>	<u>KSP</u>	<u>PLG</u>	<u>QTZ</u>	<u>HB</u>	<u>BIO</u>	<u>CHL</u>	<u>EPI</u>	<u>.CPX</u>	<u>SER</u>	<u>SPH</u>	<u>ZIR</u>	<u>APA</u>	<u>MAG</u>	<u>OTHER</u>
19	Ho,Hy,P,My	33	25	15	12	7	5	1		3	1	Tr	Tr	2	1 CAL
273	Ho,Hy	32	25	12	6	8	6	2		4	Tr	Tr	1	3	
338	Ho,Hy,P	28	26	14	10	8	5	1	2	3	Tr	Tr	1	2	
359	Ho,Hy	35	28	16	5	6	3	2	1		1	Tr	Tr	3	
368	Ho,Hy,P	34	27	10	6	5	8	1	Tr	Tr	1	Tr	Tr	3	
390	Ho,Hy	20	30	30	5	2.5	2.5	3	3	Tr	Tr		1	2	
605	P,Ho,Hy	30	26	15	8	9	6	Tr	1		1	Tr	1	2	
9-A 607	Ho,Hy	20	40	12	8	8	6	Tr		2	2	Tr	.5	2	Tr CAL
611	Ho,Hy	18	10	10	2			1	52		1		3		

TABLE IX. Modal Compositions of Quartz Porphyry Dike

<u>T.S.#</u>	<u>TEXTURE</u>	PHENOCRYSTS							<u>QTZ</u>	<u>KSP</u>	<u>CAL</u>	<u>CHL</u>	<u>APA</u>	<u>ZIR</u>	<u>SER</u>	<u>OTHER</u>
		<u>QTZ</u>	<u>PLG</u>	<u>KSP</u>	<u>SPH</u>	<u>MUS</u>	<u>OTHER</u>									
213	P	14	5	7	.5		3 BIO	68				Tr	Tr		2 BIO	
235			18	10			2 CAL	65		3	1	.5	Tr			
237	P	5	6	1	1		2 CHL	80			5					
312	Ft	8		4		1	Tr CAL	38	44					5		
352	P	10		5		1	Tr MAG	80						4		
391		7		3		2		68						2	Tr MAG	
460		6	5	1		1		72				Tr	Tr	10	5 LIM	

TABLE X. Modal Compositions of Andesite Dikes

A-7

<u>T.S.#</u>	<u>TEXTURE</u>	<u>CPX</u>	<u>PLG</u>	<u>QTZ</u>	<u>HB</u>	<u>CHL</u>	<u>EPI</u>	<u>MAG</u>	<u>CAL</u>	<u>APA</u>
177	Sk,P	20	16	7	10	15	12	16	4	1
325	Sk	41	15	4	14	8	15	2	0	1

TABLE XI. Modal Compositions of Olivine Basalt

<u>T.S.#</u>	<u>TEXTURE</u>	PHENOCRYSTS						<u>DIVT GLASS</u>
		<u>OLI</u>	<u>PLG</u>	<u>OLI</u>	<u>CPX</u>	<u>BIO</u>	<u>MAG</u>	
274	Ft	5	60	12	12	2	4	5
469	Ft	8	52	10	14	1	5	10

TABLE XII. Modal Compositions of Other Intrusives

ALASKITE

<u>T.S.#</u>	<u>TEXTURE</u>	<u>MIC</u>	<u>PLG</u>	<u>QTZ</u>	<u>KSP</u>	<u>BIO</u>	<u>CHL</u>	<u>APA</u>	<u>SPH</u>	<u>SER</u>
380	Ho	30	15	30	18	3.5	3.5	Tr	Tr	Tr

GRANOPHYRIC GRANITE

<u>T.S.#</u>	<u>TEXTURE</u>	<u>KSP</u>	<u>QTZ</u>	<u>SPH</u>
358	Ho,Gr,My	44	45	1

PERTHITIC AUGITE SYENITE

<u>T.S.#</u>	<u>TEXTURE</u>	<u>KSP</u>	<u>PLG</u>	<u>AUG</u>	<u>SPH</u>	<u>APA</u>	<u>MAG</u>
241	Ho,P	45	9	39	2	3	2

APPENDIX B. Modal Compositions of Ore Samples

The following table gives the modal compositions and textures observed in polished section.

<u>Mineral</u>	<u>Abbreviation</u>
Bornite	BOR
Chalocite	CAC
Chalcopyrite	CPY
Covellite	COV
Digenite	DIG
Galena	GAL
Malachite	MAL
Native Silver	NS
Pyrite	PY
Sphalerite	SPH
Stromeyerite	STR
Tetrahedrite	TET

<u>Texture</u>	<u>Abbreviation</u>
Exsolution	EX
Fibrous	FI
Granular Aggregates	GA
Spherical Blebs	SB
Triangular Pitted	TP
Twinning Lamellae	TL
Vein	V

Modal values are estimated and listed in percent (%).

TABLE XIII. Modal Compositions of Polished Ore Samples

<u>P.S.#</u>	<u>TEXTURE</u>	<u>GAL</u>	<u>TET</u>	<u>COV</u>	<u>CAC</u>	<u>SPH</u>	<u>CPY</u>	<u>PY</u>	<u>BOR</u>	<u>OTHER</u>	<u>GANGUE</u>
MDD 1	Ex,Ga,Tp	82	3	1	1	2	Tr	10			
MDD 2	Tp,Sb	95	4	1							
MDD 603A	Ex,Ga,Tp	82	1	1		1	Tr-1	11	Tr		3
MDM 525	Ex,Fi	72	3	2	6	6					11
MDM 570	Ex,Tl,Fi	84	2	1	2	1					10
MDM 572	Ex,Sb	94	3	.5	.5	1				Tr DIG, STR,MAL	
MDM 578	V,Ga,Tp	95	3	1						Tr NS	4
MDM 580	Fi	87	1	1							1
MDM 582A	Tp,Fi	94	3	.5	.5						
MDM 598	Ex,Ga,Tp	88	4	1	Tr	1	Tr	4	Tr		Tr

A-10.

APPENDIX C. Analyses of Assayed Samples

(Sample locations are plotted on Plate 1)

SAMPLE #	Au	Ag	Cu	Pb	Zn	Mn
5051	0.0146	4.228	378.3	12000	97800	3780
5052	0.0015	0.029	21.5	346.0	421.0	238.2
5053	0.0154	0.759	1765	21600	6770	30410
5054	0.0048	1.279	1472	4600	6730	13010
5055	0.0094	4.538	3071	19100	32100	24750
5056	0.0059	0.785	367.2	9400	5780	26210
5057	0.0090	0.388	325.1	5800	3080	10430
5058	0.0016	1.042	834.0	1010	542.0	423.0
5059	0.0500	140.4	30380	16800	2670	220.6
5060	0.0015	0.005	18.3	136.0	44.5	135.9
5061	0.0023	0.447	183.4	1860	1566	5720
5062	0.0030	0.120	139.8	10600	8690	5950
5063	0.0066	0.558	495.6	12800	3950	25820
5064	0.0018	0.684	3118	12200	15390	20760
5065	0.0055	0.015	124.3	41.8	30.1	
5066	0.0112	0.407	16550	100.0	407.0	3470
5067	0.0019	0.012	11.4	516.0	151.1	
5068	0.0071	0.072	146.6	40.3	27.7	
5069	0.0015	0.005	41.6	326.0	141.6	
5070	0.0015	0.009	145.7	189.7	224.7	
5071	0.0015	0.009	23.0	189.6	42.5	
5072	0.0015	0.007	100.7	150.6	250.0	
5073	0.0015	0.005	77.6	98.7	173.0	
5074	0.0015	0.008	6.0	54.7	74.6	
5075	0.0036	3.737	61.6	14550	20260	
5076	0.0020	0.005	8.5	31.3	24.7	
5077	0.0015	0.016	112.8	62.2	41.4	
5078	0.0015	0.005	82.3	17.7	35.5	
5079	0.0015	0.007	46.1	22.1	64.4	
5080	0.0015	0.096	19.1	18.7	51.4	
5081	0.0015	0.053	64.9	30.6	26.8	
5082	0.0015	0.005	46.9	21.1	69.1	
5083	0.0037	0.023	2974	192.4	32.0	
5084	0.0020	0.163	160.0	35.9	9.3	
5085	0.0111	4.131	14620	263.7	412.0	
5086	0.0015	0.027	16.1	179.7	144.4	
5087	0.0015	0.008	40.8	162.0	95.4	
5088	0.0015	0.011	53.8	74.6	47.9	
5089	0.0015	0.005	80.8	46.6	39.6	
5090	0.0015	0.005	48.9	44.1	114.3	

Results in oz/ton: Au, Ag

Results in ppm: Cu, Pb, Zn, Mn

## APPENDIX C (Continued)

SAMPLE #	Au	Ag	Cu	Pb	Zn
5091	0.0055	9.899	1121	19120	25000
5092	0.0015	0.005	3.2	12.2	11.9
5093	0.0015	0.006	51.5	22.7	174.2
5094	0.0015	0.007	10.8	10.4	20.5
5095	0.0015	0.005	75.1	17.0	220.3
5096	0.0015	0.010	164.9	15.4	22.4
5097	0.0015	0.014	77.8	43.1	158.9
5098	0.0015	0.008	66.1	57.8	69.7
5099	0.0040	0.358	272.3	2102	366.6
5100	0.0180	0.200	359.0	1522	345.9
5101	0.0015	0.005	23.5	17.4	461.7
5102	0.0107	0.759	123.4	192.6	30.2
5103	0.0015	0.005	70.8	27.0	59.8
5104	0.0015	0.005	103.0	10.9	38.3
5105	0.0015	0.005	63.3	15.3	1.1
5106	0.0015	0.033	20.2	12.8	12.7
5107	0.0015	0.046	129.0	257.1	144.6
5108	0.0015	0.005	80.2	34.5	57.9
5109	0.0015	0.005	11.2	50.3	209.1
5110	0.0015	0.058	13.7	22.6	136.2
5111	0.0015	0.041	51.8	18.6	18.6
5112	0.0015	0.644	28.0	23.7	17.9
5113	0.0015	0.011	104.6	37.2	41.6
5114	0.0015	0.005	3.5	29.6	41.5
5115	0.0015	0.007	6.8	44.9	70.3
5116	0.0015	0.063	8.3	41.9	49.9
5117	0.0120	0.005	8.1	65.5	75.8
5118	0.0015	0.020	3.9	27.8	31.0
5119	0.0015	0.013	8.4	41.4	50.1
5120	0.0015	0.005	8.2	32.4	30.0
5121	0.0015	0.629	138.4	53.5	120.1
5122	0.0015	0.005	132.1	15.0	43.4
5123	0.0015	0.032		153.6	
5124	0.0034	0.009	37.5	61.3	74.1
5125	0.0015	0.045		49.2	
5126	0.0015	0.021	65.9	96.6	322.9
5127	0.0015	0.011		25.7	
5128	0.0015	0.949		676.0	
5129	0.0015	0.013		59.4	
5130	0.0015	0.007		32.6	
5131	0.0015	0.017		119.3	
5132	0.0015	0.016		104.2	
5133	0.0015	0.012		32.0	

## APPENDIX C (Continued)

SAMPLE #	Au	Ag	Cu	Pb
5134	0.0015	0.012		24.0
5135	0.0235	0.100		16.1
5136	0.0446	4.488		8960
5137	0.0037	0.011		53.5
5138	0.0018	0.475		73.6
5139	0.0355	0.026		74.5
5140	0.0019	0.008		66.4
5141	0.0021	0.642		105.8
5142	0.0019	0.364		50.3
5143	0.0270	0.006		14.1
5144	0.0052	0.025		101.7
5145	0.0016	0.006		49.0
5146	0.0015	0.005		19.7
5147	0.0015	0.006		14.2
5148	0.0015	0.006		18.2
5149	0.0015	0.006		28.5
5150	0.0015	0.004		33.2
5151	0.0015	0.006		30.4
5152	0.0015	0.045		53.5
5153	0.0015	0.006		85.8
5154	0.0015	0.008		135.3
5155	0.0015	0.005		37.6
5156	0.0015	0.005		535.0
5157	0.0015	0.005		46.4
5158	0.0015	0.005		24.6
5159	0.0028	0.987		8060
5160	0.0015	0.005		216.0
5161	0.0015	0.006		88.0
5162	0.0032	0.017		94.8
5163	0.0066	0.010		48.7
5164	0.0015	0.005		24.9
5165	0.0466	14.067		14710



APPENDIX D. Table XIV Chemical Analyses of Igneous Rocks

	<u>SiO2</u>	<u>Al2O3</u>	<u>MgO</u>	<u>K2O</u>	<u>Na2O</u>	<u>Fe2O3*</u>	<u>MnO</u>	<u>Ba</u>	<u>TiO2</u>	<u>P2O5</u>	<u>CaO</u>	<u>Total**</u>
<u>NON-ALTERED QUARTZ MONZONITE</u>												
273	65.74	16.74	1.98	3.55	2.78	1.54	.09	.07	.53	.27	6.7	100.00
359	62.50	16.74	1.94	4.12	2.83	5.76	.14	.08	.67	.44	4.75	100.00
390	62.50	17.34	1.74	4.45	2.82	4.88	.15	.09	.60	.46	4.9	100.00
605	61.79	17.29	2.09	4.57	2.71	5.50	.16	.09	.67	.43	4.71	100.00
607	61.20	17.30	1.89	4.50	2.60	5.75	.15	.08	.70	.41	5.44	100.00
<u>ALTERED QUARTZ MONZONITE</u>												
611	49.94	10.90	10.80	1.29	1.50	5.55	.15	.02	.36	1.82	17.6	100.00
<u>ALASKITE APLITE</u>												
380	73.23	14.73	0.35	6.39	2.74	1.11	.03	.04	.14	.06	1.18	100.00
<u>QUARTZ PORPHYRY</u>												
312	74.39	14.93	0.37	5.10	2.72	0.92	.03	.06	.12	.04	1.33	100.00
<u>ANDESITE DIKE</u>												
325	57.95	18.33	2.0	5.82	3.34	5.14	.13	.11	.71	.61	5.86	100.00
<u>OLIVINE BASALT</u>												
469	47.55	13.53	7.56	2.03	1.76	14.22	.20	.07	1.65	.67	10.76	100.00

\* Fe2O3 is total Fe

\*\* Weight % recalculated to 100%